MODES OF OPTICAL WAVEGUIDES

by

William R. Young

A thesis submitted to the Australian National University in March 1978 for the degree of Master of Science.

PREFACE

This thesis is a report of work carried out in the Department of Applied Mathematics, Research School of Physical Science, Australian National University between January and August 1977.

The results in this thesis are original, in the sense that they are the product of a close collaboration between myself and my supervisor Allan Snyder. These results are also being reported in a paper entitled "Modes of Optical Waveguides" which has been accepted by the Journal of the Optical Society of America.

_____

William R. Young

ACKNOWLEDGEMENTS

No acknowledgement can express sufficient gratitude to my supervisor Allan Snyder. The short period of time in which this thesis was researched is adequate evidence of his industry and insight. The other members of the fiber optics group contributed to many long and illuminating discussions.

I must also thank Barry Ninham for arranging financial support. My stay in his department was a stimulating and enjoyable introduction to the scientific profession.

ABSTRACT

This thesis develops a method for finding the modes of optical waveguides with a cladding refractive index that differs only slightly from the refractive index of the core. The method applies to waveguides of arbitrary refractive index profile, arbitrary number of propagating modes and arbitrary cross section.

Particular problems investigated include the consequences of a small elliptic deformation of the core of a circular step index fiber. Only a minute eccentricity is necessary for the well known LP modes to be stable on an elliptical core.

CONTENTS

CHAPTER 1

PRELIMINARIES

1.1 Introduction

The optical fibers used in communications technology[1,2] and the optical fibers which form the retinas of verterbrate eyes[3,4] have a cladding refractive index, n_{cl}, that differs only slightly from the maximum refractive index of the core, n_{co} (see Figure 1). This observation has important theoretical consequences; previously it has been used to substantially simplify the modal fields and the eigenvalue equation of a step index circular fiber.[1] The simplification achieved in this particular problem is one of the most important theoretical advances in fiber optics.

In this thesis I shall present a simple method for determining the bound modes of any $n_{co} \cong n_{cl}$ waveguide. This procedure, called the $n_{co} \cong n_{cl}$ method, applies to $n_{co} \cong n_{cl}$ waveguides of arbitrary cross section and profile grading. It is a generalisation of the $n_{co} \cong n_{cl}$ approximation of the bound modes of the step index circular fiber[1] and provides results consistent with the properties of graded profiles previously reported.[5-7] Besides being applicable to a much wider class of fibers, the $n_{co} \cong n_{cl}$ method also clarifies the physical principles underlying the mathematical simplifications which occur when $n_{co} \cong n_{cl}$.

From a practical point of view, the most important results in this thesis are probably those concerning the consequences of a small deformation of the core of a fiber. Minuscule imperfections, such as a slightly elliptic core, are inevitable in the manufacturing process. We shall see

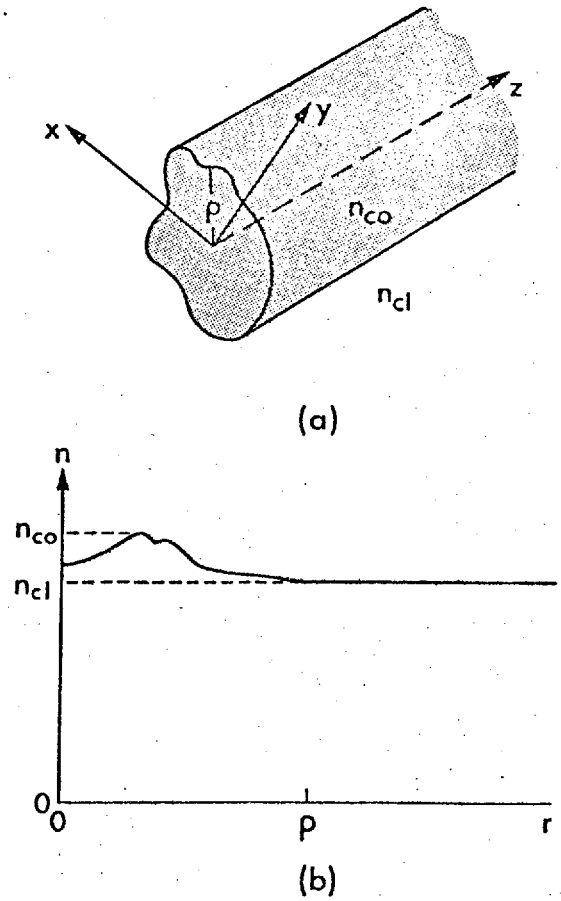

Figure 1.1: (a) A waveguide with cylindrical symmetry.

(b) The refractive index profile in some arbitrary cross section.

that small perturbations of the waveguide geometry often dramatically affect the modes of the structure.

1.2 A Review of Basic Fiber Optics

Some significant events in the history of fiber optics are summarized in Table 1.1. I shall now briefly review some fundamental concepts required for this thesis. In order to streamline the presentation the definitions of the symbols have been relegated to Table 1.2.

A mode of a cylindrical (not necessarily circular) waveguide is a field configuration which satisfies the source-free Maxwell equations and propagates unchanged except in phase (i.e., the modal fields depend on z and t only through $e^{i(\beta z-\omega t)}$). A dielectric waveguide has both a discrete set of bound modes and a continuous set of radiation modes[8]; only the bound modes are considered in this thesis. Once the modes of a structure are known a field at one position on the fiber can be expressed as a superposition of modes; the modes in the superposition then propagate individually. The modal expansion method outlined above is physically intuitive and mathematically simple, once the modes are known.

The modal electric and magnetic fields of a cylindrical waveguide (i.e., a structure whose electric permittivity $\varepsilon(x,y)$ does not depend on z) have the form

$$\underline{E}(x,y,z) = \underline{e}(x,y)e^{i\beta z} = (\underline{e}_t + \underline{e}_z)e^{i\beta z} \tag{1.1}$$

$$\underline{H}(x,y,z) = \underline{h}(x,y)e^{i\beta z} = (\underline{h}_t + \underline{h}_z)e^{i\beta z} \tag{1.2}$$

Table 1.1: Significant Events in the History of Fiber Optics.

Date	Event
1730	Newton's speculation on Goos Hänchen shift.[9]
1897	Rayleigh's investigation of the modes of a dielectric cylinder.[10]
1936	Carson, Mead and Schelkunoff consider using dielectric cylinders as microwave waveguides.[11]
1948	Toraldo di Francia suggests an explanation of the Stiles-Crawford effect, based on the acceptance properties of optical fibers.[19]
1949	Chandler demonstrates experimentally that dielectric cylinders guide more energy around a bend than metal waveguides.[12] Adler investigates the general properties of inhomogeneous dielectric cylinders.[8]
1951	Kapany and van Heal develop the cladded fiber.[13]
1958	Schawlow and Townes propose the laser.[14]
1961	Snitzer develops a losing fiber. Snitzer and Osterberg observe isolated modes on fibers.[15,16] Enoch shows that retinas are optical fiber bundles.[17,3]
1966	Kayo and Hockam suggest that dielectric rods are a practical way of transmitting information.[18]
1969	Snyder simplifies the modes and eigenequation of a step index circular fiber using $n_{co} \cong n_{cl}$ approximation.[1]
1970-75	Development of fibers with low material loss.[20-22]

Table 1.2: Glossary of Symbols

Symbol	First Occurrence (page #)	Meaning and other useful information
n_{cl}	7	Refractive index of the cladding.
n_{co}	7	Maximum refractive index of the core.
β	8	Modal propagation constant.
ω	8	Radian frequency.
$\underline{E}$ & $\underline{H}$	8	Generic symbols of electric and magnetic fields.
$\underline{e}$ & $\underline{h}$	8	Modal electric and magnetic fields.
$\underline{e}_t$ & $\underline{h}_t$	8	Transverse modal fields.
$\underline{e}_z$ & $\underline{h}_z$	8	Longitudinal modal fields.
∇_t^2	13	Transverse vector Laplacian.
$\underline{\nabla}_t$	13	Transverse differential operator.
$k(x,y)$	13	Local wavenumber, $k(x,y) = \omega(\mu\varepsilon(x,y)^{1/2} = 2\pi n(x,y)/\lambda$.
$\varepsilon(x,y)$	13	Electric permittivity.
μ	13	Magnetic permeability.
$n(x,y)$	13	Local refractive index.
λ	13	Wavelength.
ε_o	13	Permittivity of free space, $\varepsilon(x,y) = \varepsilon_o n^2(x,y)$.
k_{co} and k_{cl}	13	$k_{co} = 2\pi n_{co}/\lambda$ and $k_{cl} = 2\pi n_{cl}/\lambda$.
p	13	Modal power.
δ_{ij}	14	$\delta_{ij} = \begin{cases} 1 \text{ if } i = j \\ 0 \text{ otherwise} \end{cases}$.

Table 1.2: continued

Symbol	First Occurrence (page #)	Meaning and other useful information
A_∞	14	The Transverse plane.
η	14	Fraction of modal power in the core.
v_g	14	Modal group velocity
W	14	Modal energy stored per unit length.
θ_c^2	14	$\theta_c^2 = 1 - (n_{co}/n_{cl})^2$.
v	18	$v = \{k_{co}^2 - k_{cl}^2\}^{1/2} = (2\pi/\lambda)\{n_{co}^2 - n_{cl}^2\}^{1/2}$.
ρ	19	Radius of a circular fiber.
V	19	Waveguide parameter of a circular fiber.
$\sim$	19	Denotes quantities associated with the $n_{co} = n_{cl}$ waveguide.
ψ	20	Solution of the scalar wave equation.
ρ_{co}	20	Characteristic length of a fiber cross section.
$\hat{n}$	23	Outward unit normal of the core-cladding interface of a step-index fiber.
a_n	23	Generic symbol for coefficients in a linear combinations.
C_{ij}	23	Generic symbol for elements of a perturbation matrix.
ψ_e, ψ_o	29	Even and odd solutions of the scalar wave equation.

Table 1.2: continued

Symbol	First Occurrence (page #)	Meaning and other useful information
$f_\ell(r)$	29	Generic symbol for radial dependence function of a circular waveguide.
$\underline{\tilde{e}}_{xe}, \underline{\tilde{e}}_{xo}$ $\underline{\tilde{e}}_{ye}, \underline{\tilde{e}}_{yo}$	29	Generic symbol for transverse $n_{co} = n_{cl}$ modal electric fields of a circular waveguide.
ℓ	29	Azimuthal wavenumber.
$\underline{e}_{t1}, \underline{e}_{t2}$ $\underline{e}_{t3}, \underline{e}_{t4}$	31 & 32	Generic symbol for transverse $n_{co} \cong n_{cl}$ modal electric fields of a circular waveguide.
β_{HE} and β_{EH}	34	Propagation constants of modes 2,3 and modes 1,4 respectively.
$\tilde{\beta}_e, \tilde{\beta}_o$	35	Progagations constants of even and odd solutions of the scalar wave equation.
Λ	35	Generic symbol for the parameter which determines the composition of a mode.
$\tilde{U}, \tilde{W}$	39	Normalised transverse wavenumbers of a circular fiber.
J_ℓ, K_ℓ, I_ℓ	39 & 45	Standard symbols for Bessel functions.
e	Fig. 3.3	Eccentricity of an ellipse, $e = \sqrt{1 - (\frac{\text{minor axis}}{\text{major axis}})^2}$
$\psi_\pm$	46	Symmetric and antisymmetric solutions of the scalar wave equation for two parallel waveguides.

(see Table 1.2). The field $\underline{e}_t(x,y)$ is a solution of the reduced wave equation

$$\nabla_t^2 \underline{e}_t + (k^2-\beta^2)\underline{e}_t = -\underline{\nabla}_t(\underline{e}_t \cdot \nabla_t \ell n\varepsilon) \tag{1.3}$$

where ∇_t^2 is the transverse vector Laplacian.[23] The local wavenumber $k(x,y)$, electric permittivity $\varepsilon(x,y)$ and refractive index are related by

$$k(x,y) = \omega(\mu\varepsilon(x,y))^{1/2} = 2\pi n(x,y)/\lambda \tag{1.4}$$

and

$$\varepsilon(x,y) = \varepsilon_o n^2(x,y) \tag{1.5}$$

(see Table 1.2). The remaining field components are determined from $\underline{e}_t$ using Maxwell's equations. The allowed values of β result by demanding only that the solutions of equation 1.3 be bounded, since effects of any discontinuities in ε are fully contained within the $\underline{\nabla}_t \ell n\varepsilon$ term. For bound modes β is real and restricted to the range[8]

$$k_{cl} \leq \beta \leq k_{co} \quad . \tag{1.6}$$

The modal fields are in general hybrid possessing both $\underline{e}_z$ and $\underline{h}_z$ components.[8] Furthermore, for the bound modes of a lossless structure the normalisation can be chosen so that $\underline{e}_t, \underline{h}_t$ are real, while $\underline{e}_z, \underline{h}_z$ are imaginary. The time averaged power of a mode is

$$p = 1/2 \int_{A_\infty} \underline{e} \times \underline{h}^* \cdot \hat{\underline{z}} \, dA \tag{1.7}$$

where * is complex conjugate, and A_∞ is the infinite cross section. The bound modes of a lossless structure obey power orthogonality[8]

$$\int_{A_\infty} \underline{e}_i \times h_j^* \cdot \hat{z}\, dA = 2p\delta_{ij} \tag{1.8}$$

where p is equation 1.7 and δ_{ij} is the Kronecker delta. Not all the power in a waveguide is transmitted within the core, only a fraction

$$\eta = \int_{core} \underline{e} \times h^* \cdot \hat{z}\, dA / \int_{A_\infty} \underline{e} \times h^* \cdot \hat{z}\, dA \tag{1.9}$$

is carried within the core. The group velocity of a mode is

$$v_g = \partial\omega/\partial\beta = 4p/W \tag{1.10}$$

where W, the stored energy per unit length, it

$$W = \int_{A_\infty} \{\varepsilon|\underline{e}|^2 + \mu|\underline{h}|^2 + \omega|\underline{e}|^2(d\varepsilon/d\omega)\}dA \ . \tag{1.11}$$

The reason for having a small difference between n_{co} and n_{cl} in communications technology is that delay distortion (derivative of group velocity with respect to frequency) is proportion to

$$\theta_c^2 = 1 - (n_{co}^2/n_{cl}^2) \ . \tag{1.12}$$

Bibliography and Footnotes for Chapter 1

1. A.W. Snyder, "Asymptotic expressions for eigenfunctions and eigenvalues of a dielectric or optical waveguide," IEEE MTT-17 (12), 1130-1138 (1969).
2. P.J.B. Clarricoats, "Theory of optical fiber waveguides: A review" in Progress in Optics, Vol. 14, E. Wolf (ed.), (North-Holland, Amsterdam, 1976).
3. J.M. Enoch, "Nature of the transmission of energy in the retinal receptors," J. Opt. Soc. Am. 51, 1122-1126 (1961).
4. A.W. Snyder and R. Menzel (eds.), Photoreceptor Optics (Springer-Verlag, Berlin, 1975).
5. R. Yamada and Y. Inabe, "Guided waves in an optical square-law medium," J. Opt. Soc. Am. 64, 964-969 (1974).
6. J.O. Koshi and K. Okamoto, "Analysis of wave propagation in inhomogeneous optical fibers using a variational method," IEEE trans. MTT 22, 938-945 (1974).
7. C.N. Kurtz, "Scalar and vector mode relations in gradient-index light guides," J. Opt. Soc. Am. 65, 1235-1240 (1975). This paper is specialised to waveguides of circular symmetry. The vector Laplacian ∇_t^2 is expressed in cylindrical coordinates and the $\underline{\nabla}_t \ell n \varepsilon$ term is neglected. Solutions of this equation automatically obey the correct symmetry properties of the structure because the vector Laplacian has been written in cylindrical coordinates.
8. R.B. Adler, "Properties of guided waves on inhomogeneous cylindrical structures," M.I.T. Research Lab. of Electronics, Tech. Report 102 (1949). (Summarised in "Waves on inhomogeneous cylindrical structures,"

Proc. I.R.E. 40, 339-348 (1952).)

9. I. Newton, Opticks, 4th edition (1730), Query 20 [Reprinted by Dover, New York, 1952].
10. Lord Rayleigh, "Vibrations in dielectric cylinders," Phil. Mag. 43 (125), (1897).
11. J. Carson, S. Mead, S. Schelkunoff, "Hyper-frequency waveguides - mathematical theory," BSTJ 15 (1936).
12. C.H. Chandler, "An investigation of dielectric rods as waveguides," J. Appl. Phys. 20 (1949).
13. N.S. Kapany and J. Burke, "Fiber optics.IX waveguide effects," J. Opt. Soc. Am. 51, 1067-1078 (1961).
14. A.L. Schawlow and C.H. Townes, "Infrared and optical masers," Phys. Rev. 112 (1958).
15. E. Snitzer, "Cylindrical dielectric waveguide modes," J. Opt. Soc. Am. 51, 491-498 (1961).
16. E. Snitzer and H. Osterberg, "Observed dielectric waveguide modes on the visible spectrum," J. Opt. Soc. Am. 51, 499-505 (1961).
17. J.M. Enoch, "Optical properties of the retinal receptors," J. Opt. Soc. Am. 53, 71-85 (1963).
18. K.C. Kao and G.A. Hockham, "Dielectric-fiber surface waveguides for optical waveguide," Proc. IEE 113 (7), 1151 (1966).
19. G. Toraldo di Francia, "Per una teoria dell'effecto Stiles-Crawford," Il Nuovo Cimento (9) 5, 589-590 (1948).
20. F.P. Kapron, D.B. Keck and R.D. Maurer, "Radiation losses in glass optical waveguides," Appl. Phys. Lett. 10, 423-425 (1970).

21. D.N. Payne and W.A. Gambling, "New silica-based low-loss optical fibre," Electron. Lett. 10, 289-290 (1974).

22. W.G. French and G.W. Tasker, "Fabrication of graded index and single mode fibers with silica cores," Paper TuA2, O.S.A./IEEE Meeting on Optical Fiber Transmission, Williamsburg, 1975.

23. P.M. Morse and H. Feshbach, Methods of Theoretical Physics, McGraw-Hill, New York (1953), p. 116.

CHAPTER 2

THE $n_{co} \cong n_{cl}$ METHOD

In this chapter I present the $n_{co} \cong n_{cl}$ method. This procedure synthesises the vector modal fields of the $n_{co} \cong n_{cl}$ waveguide from linear combinations of solutions of the scalar wave equation. The appropriate linear combinations are dictated by properties of the $\underline{\nabla}_t \ell n \varepsilon$ term in equation 1.3. Failure to account for the effects of the $\underline{\nabla}_t \ell n \varepsilon$ term, however small, leads to the well known LP or $n_{co} = n_{cl}$ modes.[1] The cross sectional intensity and polarisation pattern of the $n_{co} = n_{cl}$ modes changes as the modes propagate.[1,2,8,9]

2.1 The $n_{co} = n_{cl}$ Waveguide - No Polarisation Properties

We begin by finding the modes of a waveguide in the artificial limit

$$n_{co} \to n_{cl} = n \quad \text{or equivalently} \quad \theta_c \to 0 \qquad (2.1)$$

which, by itself, amounts to assuming that the medium is homogeneous, without the capacity to guide waves. To avoid the trivial consequences of this limit, we impose the crucial constraint that $\lambda \to 0$ in such a way that the parameter

$$v = \{k_{co}^2 - k_{cl}^2\}^{1/2} = 2\pi/\lambda\{n_{co}^2 - n_{cl}^2\}^{1/2} = k_{co}\theta_c \qquad (2.2)$$

equals an arbitrary constant. This second constraint ensures that the structure guides waves. A similar approach is used in deriving the modes of a circular step index waveguide,[3] in which the waveguide parameter V is held

constant,

$$V = \rho(k_{co}^2 - k_{cl}^2)^{1/2} \tag{2.3}$$

where ρ is the core radius. In other words by holding v constant and letting $n_{co} \to n_{cl}$ (or equivalently, $\theta_c \to 0$) the waveguide is not merely a homogeneous medium.[10] We now investigate the properties of the bound modes on this $n_{co} = n_{cl}$ waveguide, anticipating that these modes should have some properties in common with modes of the $n_{co} \cong n_{cl}$ waveguide.

Because the β of a bound mode is restricted to the range of values in equation 1.6, the limit $n_{co} = n_{cl}$ demands that

$$\beta \to k_{co} \to k_{cl} \to \infty \quad . \tag{2.4}$$

This condition is satisfied only by a z-directed transverse electromagnetic (TEM) wave, i.e., a wave for which the electric and magnetic field vectors lie in a plane that is transverse to the axis of the waveguide. Accordingly, the modal fields of the $n_{co} = n_{cl}$ waveguide satisfy

$$\tilde{\underline{h}}_z = \tilde{\underline{e}}_z = 0 \tag{2.5}$$

$$\tilde{\underline{h}}_t = (\varepsilon/\mu)^{1/2} \hat{\underline{z}} x \tilde{\underline{e}}_t \tag{2.6}$$

where $\tilde{}$ is used to indicate quantities associated with the $n_{co} = n_{cl}$ waveguide.

Secondly, because $n_{co} = n_{cl}$, all polarisation dependent properties of the structure are removed. If this is not

obvious, then recall that as $n_{co} \rightarrow n_{cl}$, TE and TM waves undergo identical reflection at an interface between two semi-infinite media or at a caustic.[4] Since the $\underline{\nabla}_t \ell n \varepsilon$ term in the reduced vector wave equation (1.3) is the only term which distinguishes between polarisations, it is omitted when solving for the $\underline{\tilde{e}}$ fields of the $n_{co} = n_{cl}$ waveguide. In other words, the fields of the $n_{co} = n_{cl}$ waveguide are essentially solutions of the scalar wave equation. These $n_{co} = n_{cl}$ or LP modal fields are expressed in rectangular coordinates as

$$\underline{\tilde{e}}_x = \psi \underline{\hat{x}} \tag{2.7a}$$

$$\underline{\tilde{e}}_y = \psi \underline{\hat{y}} \tag{2.7b}$$

where ψ is a solution of

$$\{\nabla_t^2 + (k^2 - \tilde{\beta}^2)\}\psi = 0 \tag{2.8}$$

and ∇_t^2 is the transverse portion of the scalar Laplacian operator.[11] The solution ψ must be bounded everywhere and have the well known property of the scalar wave equation that ψ and its normal derivative are continuous everywhere, even if $k^2(x,y)$ is discontinuous. These constraints lead to an eigenvalue equation from which the allowed values of $\tilde{\beta}$ are found. We anticipate that these values of $\tilde{\beta}$ are nearly equal to k. Furthermore, as $n_{co} \rightarrow n_{cl}$, $\rho_{co}\beta$ becomes arbitrarily large, where ρ_{co} is a characteristic length of the cross section.

In conclusion, the $n_{co} = n_{cl}$ waveguide was invented to physically motivate the introduction of the $n_{co} = n_{cl}$ fields in equation 2.7. It is important to realise that the $n_{co} = n_{cl}$ waveguide has no polarisation dependent properties i.e., the $n_{co} = n_{cl}$ waveguide has no preferred direction for the electric field of a mode.[12] Notice also that nowhere in this section has an appeal been made to the often quoted condition that

$$|\lambda \nabla_t \varepsilon/\varepsilon| << 1 \ . \qquad (2.9)$$

All that has been used is $n_{co} \cong n_{cl}$.

2.2 The $n_{co} \cong n_{cl}$ Waveguide-Inclusion of Polarisation Properties

The significant consequence of having n_{co} different from n_{cl} is that the waveguide has polarisation properties. The polarisation properties are contained within the $\nabla_t \ell n \varepsilon$ terms of the vector wave equation. The modes of an $n_{co} \cong n_{cl}$ waveguide are solutions of the vector wave equation and therefore have polarisation properties. However, since the term $\nabla_t(\underline{e}_t \cdot \nabla_t \ell n \varepsilon)$ is zero when $n_{co} = n_{cl}$, it must be small when $n_{co} \cong n_{cl}$.[13] Hence, the modes of the $n_{co} \cong n_{cl}$ waveguide can be approximated by finite linear combinations of the $n_{co} = n_{cl}$ modal fields.

From a mathematical point of view, the $n_{co} \cong n_{cl}$ method is a variant of the familiar Rayleigh-Schrödinger perturbation theory,[5-7] developed especially to treat equation 1.3 with a maximum of algebraic economy and physical insight. As a general rule in perturbation theory, unperturbed modes which

are nearly degenerate (in this particular problem, modes with nearly equal $\tilde{\beta}$'s) are "mixed" or "hybridized" by a perturbation.[14] The more nearly degenerate the modes are, the more readily they are hybridized by a perturbation. This provides one criterion for deciding which $n_{co} = n_{cl}$ modes are included in the linear combination: one combines groups of nearly degenerate modes.

In Chapter 3 I return to the problem of deciding which $\underline{\tilde{e}}$ are included in the linear combination. Frequently physical considerations enable one to eliminate some terms from the linear combination. I shall now explain how the coefficients in the linear combination are obtained, once one has decided which $n_{co} = n_{cl}$ fields are to be included.

We begin by proving an important intermediate result which relates an $n_{co} = n_{cl}$ mode to an $n_{co} \cong n_{cl}$ mode. The result is obtained by a deviation of the method used to obtain mode orthogonality. The exact field satisfies

$$\{\nabla_t^2 + (k^2-\beta^2)\}\underline{e}_t = -\nabla_t(\underline{e}_t \cdot \nabla_t \ell n\varepsilon) \tag{2.10}$$

while an $n_{co} \cong n_{cl}$ field satisfies

$$\{\nabla_t^2 + (k^2-\tilde{\beta}^2)\}\underline{\tilde{e}}_t = 0 \tag{2.11}$$

Dot product equation 2.10 with $\underline{\tilde{e}}_t$ and equation 2.11 with $\underline{e}_t$, subtract the two equations and then integrate over the plane. The term $\int_{A_\infty}\{\underline{e}_t \cdot \nabla_t^2\underline{e}_t - \underline{e}_t \cdot \nabla_t^2\underline{\tilde{e}}_t\}dA$ is converted to a line integral at infinity using the vector Green's theorem. This term vanishes since $\underline{e}_t$ and $\underline{\tilde{e}}_t$ decay exponentially. The final result is

$$\beta^2 - \tilde{\beta}^2 = \int_{A_\infty} \underline{\tilde{e}}_t \cdot \underline{\nabla}_t (\underline{e}_t \cdot \underline{\nabla}_t \ell n \varepsilon) / \int_{A_\infty} \underline{\tilde{e}}_t \cdot \underline{e}_t \, dA \qquad (2.12)$$

when $\varepsilon(x,y)$ is a step function, as in Figure 1.1, equation 2.12 can be simplified using integration by parts and

$$\underline{\nabla}_t \ell n \varepsilon \, dA = \ell n \, \varepsilon_{c1}/\varepsilon_{co} \, \delta(\text{Boundary}) \hat{n} \, d\ell \qquad (2.13a)$$

$$= -\theta_c^2 \, \delta(\text{Boundary}) \hat{n} \, d\ell \qquad (2.13b)$$

where $\hat{n}$ is the outward normal of the boundary and $d\ell$ is an elemental length at the boundary. Using equation 2.13 one has

$$\int_{A_\infty} \underline{\tilde{e}}_t \cdot \underline{\nabla}_t (\underline{e}_t \cdot \underline{\nabla}_t \ell n \varepsilon) dA = \theta_c^2 \oint_{\text{Boundary}} (\underline{\nabla}_t \cdot \underline{\tilde{e}}_t)(\underline{e}_t \cdot \hat{n}) d\ell \qquad (2.14)$$

Equation (2.12) is an exact result, no approximations have been made.

Now, suppose that one hypothesises the approximation

$$\underline{e}_t = \sum_{n=1}^{N} a_n \underline{\tilde{e}}_{tn} \, . \qquad (2.15)$$

Substitute $\underline{e}_t$ from equation 2.15 and $\underline{\tilde{e}}_t = \underline{\tilde{e}}_{ti}$ where $i = 1,\ldots,N$ into equation 2.12. After some rearranging an $N \times N$ eigenvalue equation is obtained

$$\begin{bmatrix} C_{11}+\tilde{\beta}_1^2-\beta^2 & C_{12} & C_{13} & \cdots & C_{1N} \\ C_{21} & C_{22}+\tilde{\beta}_2^2-\beta^2 & C_{23} & \cdots & C_{2N} \\ C_{31} & C_{32} & C_{33}+\tilde{\beta}_3^2-\beta^2 & \cdots & C_{3N} \\ \vdots & \vdots & \vdots & & \vdots \\ C_{N1} & C_{N2} & C_{N3} & \cdots & C_{NN}+\tilde{\beta}_N^2-\beta^2 \end{bmatrix} \begin{bmatrix} a_1 \\ a_2 \\ a_3 \\ \vdots \\ a_N \end{bmatrix} = \begin{bmatrix} 0 \\ 0 \\ 0 \\ \vdots \\ 0 \end{bmatrix} \qquad (2.16)$$

In equation 2.16, the eigenvalue is β^2, the eigenvector $[a_1, a_2, a_3, \ldots, a_N]$ and the coefficients are

$$\tilde{\beta}_i^2 = \text{propagation constant of } \underline{\tilde{e}}_{ti} \tag{2.17}$$

$$C_{ij} = \int_{A_\infty} \underline{\tilde{e}}_{ti} \cdot \nabla_t (\underline{\tilde{e}}_{tj} \cdot \nabla_t \ell n \varepsilon) \, dA / \int_{A_\infty} |\underline{\tilde{e}}_{ti}|^2 \, dA \tag{2.18}$$

The easily obtained orthogonality property

$$\int_{A_\infty} \underline{\tilde{e}}_{ti} \cdot \underline{\tilde{e}}_{tj} \, dA = 0 \tag{2.19}$$

has been used in deriving equation 2.16. The solution of our problem is effectively the eigenvalues and eigenvectors of equation 2.16.

It is usually possible to take advantage of the structure of each particular problem to simplify the procedure outlined above. In all the examples in this thesis I avoid evaluating anything more complicated than a 2×2 determinant by using physical arguments to eliminate terms in the initial linear combination equation 2.15. The details of the algebra for the 2×2 case are collected in Appendix A.

After $\underline{e}_t$ has been obtained the remaining fields are determined from Maxwell's equations. Because $\beta \cong k$ on the $n_{co} \cong n_{cl}$ waveguide, $\underline{e}_t$ and $\underline{h}_t$ are related by

$$\underline{h}_t = (\varepsilon_{co}/\mu)^{1/2} \hat{z} \times \underline{e}_t \tag{2.20}$$

The longitudinal fields are then found from Maxwell's divergence equations, leading to

$$\underline{h}_z = (i/\beta \ \underline{\nabla}_t \cdot \underline{h}_t)\hat{\underline{z}} \tag{2.21}$$

$$\underline{e}_z = (i/\beta \ \underline{\nabla}_t \cdot \underline{e}_t)\hat{\underline{z}} + 0(\theta_c^2) \ . \tag{2.22}$$

When $n_{co} \cong n_{cl}$, $\beta\rho_{co} >> 1$, so that from equations 2.20-2.22 the modes of an $n_{co} \cong n_{cl}$ waveguide are nearly TEM.

2.3 Summary

The modal fields of the $n_{co} \cong n_{cl}$ waveguide are nearly TEM waves obeying equations 2.20-2.22 with corrected propagation constants obtained by solving equation 2.16. The transverse fields are synthesised from linear combinations of the $n_{co} = n_{cl}$ fields defined in equation 2.7. In the next chapter I discuss the physical considerations which are used to simplify the mathematical prescription given above for finding $\underline{e}_t$. In particular, physically intuitive arguments can be used to eliminate some of the terms in the initial guess equation 2.15.

Bibliography and Footnotes for Chapter 2

1. D. Gloge, "Weakly guiding fibers," Appl. Opt. 10 (10), 2252-2258 (1971).
2. D. Marcuse, Theory of Dielectric Optical Waveguides, Academic Press, New York (1974).
3. A.W. Snyder, "Asymptotic expressions for eigenfunctions and eigenvalues of a dielectric or optical waveguide," IEEE MTT-17 (12), 1130-1138 (1969).
4. L.D. Landau and E.M. Lifshitz, Electrodynamics of Continuous Media, Pergamon Press (1963), p. 285.
5. Lord Rayleigh, The Theory of Sound, 2 Vols., 2nd ed., Macmillan and Co., London 1894, 1896.
6. C.A. Croxton, Introductory Eigenphysics; an approach to the theory of fields, London, New York, Wiley (1974).
7. E. Merzbacher, Quantum Mechanics, 2nd ed., Wiley (1970).
8. A.W. Snyder and C. Pask, "Light absorption in the bee photoreceptor," J. Opt. Soc. Am., 998-1008 (1972), Appendix A.
9. E. Snitzer and H. Osterberg, "Observed dielectric waveguide modes in the visual spectrum," J. Opt. Soc. Am. 51, 499-505 (1961).
10. Previous experience warns that many readers have conceptual difficulties with the limiting procedure described above. A point which must be kept in mind at all times is that despite equation 2.2, v and θ_c are independent variables. As θ_c decreases, λ decreases in such a way that v remains constant. This procedure is somewhat similar to the unphysical limit used to construct the point dipole of electrostatics. The field of a point

dipole is specified by one parameter, the dipole moment $\underline{p}$. The field of a point dipole is constructed from that of a finite dipole by an unphysical limiting procedure; the distance $\underline{d}$ between the equal and opposite charges, Q and -Q, is decreased, while Q is increased so that $\underline{p} = Q\underline{d}$ remains constant.

11. Note that equation 2.4 does not imply that $k^2 - \tilde{\beta}^2 \to 0$ in equation 2.8. It is entirely possible for, say, $x \to y \to \infty$ and yet for $x^2 - y^2$ to equal a constant (for example, if $x = \cosh t$, $y = \sinh t$ and $t \to \infty$).

12. In equations 2.7, $\hat{x}$ and $\hat{y}$ were choosen purely for convenience. Actually any two linearly independent vectors could be used to construct the $\tilde{\underline{e}}$-fields from ψ.

13. If this is not clear consider the extreme example of a step profile, where $\nabla_t \ln \varepsilon = \theta_c^2 \delta(r - \rho)$. The perturbation is zero except in a small region of space near $r = \rho$ where it has minute strength θ_c^2. When n_{co} is quite different from n_{cl}, $\nabla_t \ln \varepsilon$ is no longer small, but because it is spatially localized it is incorporated into the mathematics via the boundary conditions. In the sequel I show that the $n_{co} \cong n_{cl}$ method gives accurate results for the extreme case of a step index fiber provided $\theta_c^2 << 1$. It is important to realize that physically this is because as $n_{co} \to n_{cl}$, TE and TM waves have identical reflection properties at a caustic, no matter how rapidly the refractive index changes from n_{co} to n_{cl}.

14. The reader is reminded that the strategy of the Rayleigh-Schrodinger perturbation theory is to approximate a mode of the perturbed structure by a two or three term linear combination of unperturbed modes.

CHAPTER 3

SIMPLIFICATION OF THE $n_{co} \tilde{=} n_{cl}$ METHOD USING PHYSICAL ARGUMENTS

The philosophy of the $n_{co} \tilde{=} n_{cl}$ method, presented in Chapter 2, was to approximate an $n_{co} \tilde{=} n_{cl}$ field by a linear combination of $n_{co} = n_{cl}$ fields. The problem of finding the correct linear combinations was reduced to two steps:

a) Forming the initial linear combination equation 2.15, this necessitates deciding which modes to include.

b) Solving the eigenvalue problem equation 2.16.

Naturally the more modes which are included in step (a), the more accurate the final answer is; the price of the increased accuracy is the algebraic complexity of step (b) for $N \geq 3$. In Chapter 2 one criterion for deciding which modes to include was mentioned, viz one includes all modes which have $\tilde{\beta}$'s well separated from the $\tilde{\beta}$'s of the excluded modes. If one follows this criterion and solves equation 2.16 an answer is obtained slowly but surely. However, in many problems the final answer is simpler than the initial linear combination suggests because some of the coefficients, a_i vanish identically. In this Chapter I shall discuss the physical arguments which enable one to anticipate this simplification. Besides reducing the labour involved in solving equation 2.15 the physical insight obtained is worthwhile for its own sake.

The reasoning in this section pivots on two concepts:

a) Symmetry. If a waveguide is invariant under a geometric transformation then under the same transformation a mode of the waveguide must transform into a mode of the same β.

b) Limiting cases. By examining certain limiting cases where the correct linear combinations are known one can guess at the included modes in the linear combinations appropriate for the intermediate cases.

3.1 Waveguides with Circular Symmetry

The $n_{co} = n_{cl}$ modes are given by equation 2.7 in terms of the scalar function ψ. Because of circular symmetry, there are in general two solutions of the scalar wave equation 2.8 for each allowed value of $\tilde{\beta}$. One solution ψ_e, has even symmetry while the other, ψ_o, has odd symmetry

$$\psi_e = f_\ell(r)\cos\ell\phi \; ; \; \psi_o = f_\ell(r)\sin\ell\phi \tag{3.1}$$

In equation 3.1, ϕ is the azimuthal angle and $f_\ell(r)$ is a solution of

$$\{d^2/dr^2 + 1/r\, d/dr + k^2(r) - \tilde{\beta}^2 - \ell^2/r^2\}f_\ell(r) = 0 \tag{3.2}$$

Note when $\ell = 0$ there is only one solution of the scalar wave equation, $\psi_e(r) = f_o(r)$.

Combining the above results, the $n_{co} = n_{cl}$ waveguide in general has 4 modes for each value of $\tilde{\beta}$, i.e.,

$$\underline{\tilde{e}}_{xe} = f_\ell(r)\cos\ell\phi\ \hat{\underline{x}} \; ; \quad \underline{\tilde{e}}_{xo} = f_\ell(r)\sin\ell\phi\ \hat{\underline{x}} \tag{3.3a}$$

$$\underline{\tilde{e}}_{ye} = f_\ell(r)\cos\ell\phi\ \hat{\underline{y}} \; ; \quad \underline{\tilde{e}}_{yo} = f_\ell(r)\sin\ell\phi\ \hat{\underline{y}} \tag{3.3b}$$

I shall now discuss how to linearly combine these $n_{co} = n_{cl}$ or LP modal fields to form approximate modal fields of

the $n_{co} \cong n_{cl}$ waveguide.

1. The Fundamental ($\ell = 0$) Modes

When $\ell = 0$ there are only two $n_{co} = n_{cl}$ modes, $\underline{\tilde{e}}_{xe}$ and $\underline{\tilde{e}}_{ye}$. These two degenerate modal fields exist at all frequencies and depend only on r. The fundamental $n_{co} \cong n_{cl}$ modal fields are a linear combination of the $n_{co} = n_{cl}$ modes. From circular symmetry it is obvious that <u>any</u> linear combination of these two $n_{co} = n_{cl}$ fields is a fundamental modal field of the $n_{co} = n_{cl}$ waveguide and therefore is also a modal field of the $n_{co} \cong n_{cl}$ waveguide. In particular $\underline{e}_{xe}$ and $\underline{e}_{ye}$ are individually $n_{co} \cong n_{cl}$ modal fields:

$$\underline{e}_x = \underline{\tilde{e}}_{xe} = f_o(r)\hat{x} \; ; \; \underline{e}_y = \underline{\tilde{e}}_{ye} = f_o(r)\hat{y} \tag{3.4}$$

Circular symmetry implies that $\underline{e}_x$ and $\underline{e}_y$ are degenerate as can be verified from equation 2.12.

The two fundamental modal fields of the $n_{co} \cong n_{cl}$ waveguide are the same as the fundamental modal fields of the $n_{co} = n_{cl}$ waveguide. Note however that from equation 2.12, $\tilde{\beta} \neq \beta$, i.e., the $n_{co} = n_{cl}$ modes and $n_{co} \cong n_{cl}$ modes have different propagation constants when polarisation effects are included.

2. The Higher Order ($\ell \geq 1$) Modes

When $\ell \neq 0$ the circularly symmetric $n_{co} = n_{cl}$ waveguide has four degenerate $n_{co} = n_{cl}$ modes. Unlike the fundamental modes, none of the $\ell \geq 1$, $n_{co} = n_{cl}$ modes are modes of the $n_{co} \cong n_{cl}$ waveguide. This is proved by observing that a circularly symmetric waveguide is unchanged if it is rotated

through an arbitrary angle. Hence if a mode of the waveguide is rotated through an arbitrary angle, it must remain a mode (not necessarily the same mode) with the same β. Now, if any one of the four $n_{co} = n_{cl}$ modes in equation 3.3 is rotated through an arbitrary angle it is then represented by a linear combination of all four $n_{co} = n_{cl}$ modes.[4] Thus, if the $n_{co} = n_{cl}$ modes are also modes of the $n_{co} \cong n_{cl}$ waveguide, all four must have the same β. But if the $n_{co} = n_{cl}$ fields are substituted into equation 2.12 one finds that the four corrected $\tilde{\beta}$'s are not all equal. This contradiction between the requirements of circular symmetry and equation 2.12 proves that $n_{co} = n_{cl}$ modes are not $n_{co} \cong n_{cl}$ modes when $\ell \geq 1$. Thus, we require linear combinations of $\underline{\tilde{e}}_{xe}$, $\underline{\tilde{e}}_{xo}$, $\underline{\tilde{e}}_{ye}$, and $\underline{\tilde{e}}_{yo}$ to form higher order modes.

To form the correct linear combinations, one combines those modes which have the same properties under a rotation by 90° and under reflections in the x and y axes. (It may help at this point to consider a specific example, say the $\ell = 1$ modes shown in Figure 3.1.) Thus, $\underline{\tilde{e}}_{xe}$ is combined with $\underline{\tilde{e}}_{yo}$ because one rotates into the other, while $\underline{\tilde{e}}_{xo}$ is combined with $\underline{\tilde{e}}_{ye}$ because one rotates into minus the other. Taking symmetric and antisymmetric combinations leads to the four modes of the $n_{co} \cong n_{cl}$ waveguide:

$$\underline{e}_1 = \underline{\tilde{e}}_{xe} + \underline{\tilde{e}}_{yo} \quad ; \quad \underline{e}_2 = \underline{\tilde{e}}_{xe} - \underline{\tilde{e}}_{yo} \tag{3.5a}$$

$$\underline{e}_3 = \underline{\tilde{e}}_{xo} + \underline{\tilde{e}}_{ye} \quad ; \quad \underline{e}_4 = \underline{\tilde{e}}_{xo} - \underline{\tilde{e}}_{ye} \, . \tag{3.5b}$$

Using conventional nomenclature,[1,2] modes 1 to 4 refer to the

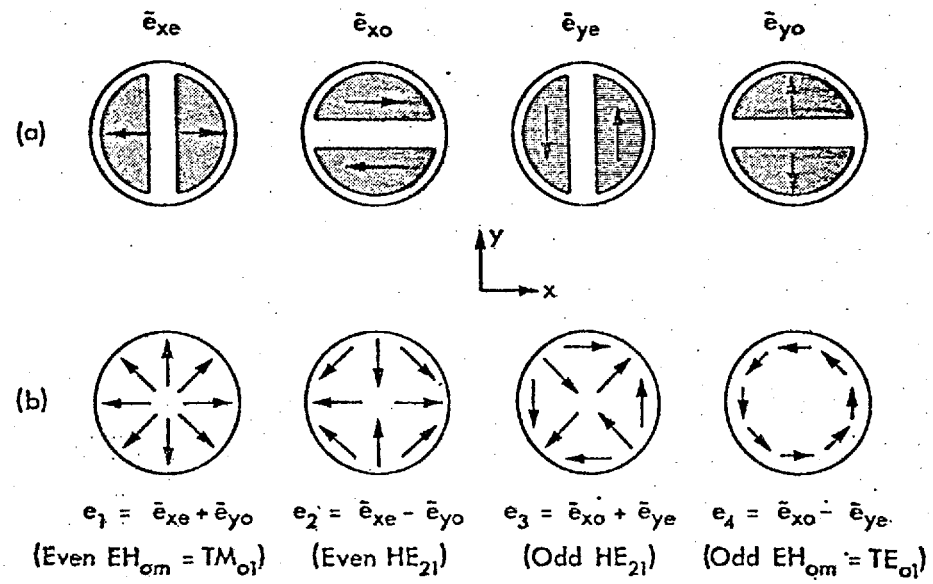

Figure 3.1: (a) The $n_{co} = n_{cl}$ or LP modes for $\ell = 1$. Note that $\underline{\tilde{e}}_{xe}$ and $\underline{\tilde{e}}_{yo}$ are symmetric under reflections in the x and y axes, while $\underline{\tilde{e}}_{xo}$ and $\underline{\tilde{e}}_{ye}$ are antisymmetric. If any one of the above fields is rotated through an arbitrary angle it transforms into a linear combination of all 4. Note also that $\underline{\tilde{e}}_{xe} = \underline{e}_1 + \underline{e}_2$, $\underline{\tilde{e}}_{xo} = \underline{e}_3 - \underline{e}_4$, $\underline{\tilde{e}}_{ye} = \underline{e}_3 + \underline{e}_4$ and $\underline{\tilde{e}}_{yo} = \underline{e}_1 - \underline{e}_2$ where the $\underline{e}$'s are shown in (b).

(b) The $n_{co} \cong n_{cl}$ modes for $\ell = 1$. Under an arbitrary reflection and rotation, $\underline{e}_1$ and $\underline{e}_4$ are unchanged while either $\underline{e}_2$ or $\underline{e}_4$ transform into linear combinations of $\underline{e}_2$ and $\underline{e}_4$.

even $EH_{\ell-1,m}$, even $HE_{\ell+1,m}$, odd $HE_{\ell+1,m}$ and odd $EH_{\ell-1,m}$ modes respectively. Figure 3.1b illustrates the modes for $\ell = 1$. These combinations are consistent with the requirements of symmetry and equation 2.12. Consider $\ell = 1$ for example. The patterns $\underline{e}_{t1}$ and $\underline{e}_{t4}$ of Figure 3.1 are unchanged by reflection in an arbitrary axis and by rotation through an arbitrary angle, consistent with their being nondegenerate modes of a circularly symmetric waveguide. However, under arbitrary rotation and reflections $\underline{e}_{t2}$ changes into a linear combination of $\underline{e}_{t2}$ and $\underline{e}_{t3}$. Symmetry demands that this new combination is also a mode, which in turn requires that $\underline{e}_{t2}$ and $\underline{e}_{t3}$ are degenerate. This is consistent with the results of equation 2.12. Analogous arguments show that the linear combinations in equation 3.5 are consistent also when $\ell \neq 1$; one finds that $\underline{e}_{t1}$ is degenerate with $\underline{e}_{t4}$ and $\underline{e}_{t2}$ is degenerate with $\underline{e}_{t3}$.

The difference in the modal propagation constants gives rise to a beat phenomenon causing a rotation of the $n_{co} = n_{cl}$ or LP patterns. The stability of the LP mode patterns is set by the difference $\beta_{HE} - \beta_{EH}$ in the propagation constants of the constituent modes of an LP pattern. When the difference is large an LP pattern rotates rapidly, when it is zero the LP modes are also modes of the $n_{co} \cong n_{cl}$ waveguide.

3.2 Waveguides with Two Preferred Axes of Symmetry

Many structures of practical interest have a pair of preferred orthogonal axes of symmetry, e.g., the ellipse and composite two cylinder waveguide of Figure 3.2. When $n_{co} \cong n_{cl}$, the modes of the waveguides can be formed by linear

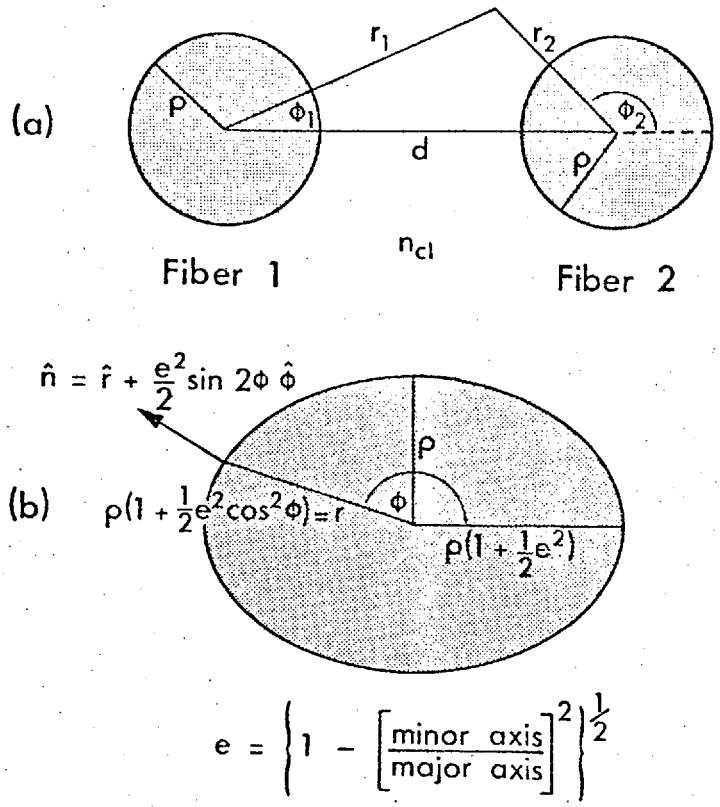

Figure 3.2: Waveguides with preferred axes of symmetry. (a) Composite, two parallel waveguide system, and (b) an Elliptical core.

combinations of $n_{co} \cong n_{cl}$ modal fields. I now show how to form these linear combinations, beginning with the fundamental modes.

1. The Fundamental Modes

It is intuitive that the fundamental modes, those modes which propagate for all frequencies, have electric fields that are polarised along one of the two axes of symmetry. Thus, the $n_{co} = n_{cl}$ or LP modal fields are the correct approximations of the fundamental fields of the $n_{co} \cong n_{cl}$ waveguide <u>provided</u> the $\hat{x}$ and $\hat{y}$ directions of equation 2.7 are aligned with the symmetry axes. Therefore, the fundamental mode has vector fields of the form

$$\underline{E}_x = \underline{e}_x e^{i\beta_x z} = \psi e^{i\beta_x z} \hat{\underline{x}} \tag{3.6a}$$

$$\underline{E}_y = \underline{e}_y e^{i\beta_y z} = \psi e^{i\beta_y z} \hat{\underline{y}} \, . \tag{3.6b}$$

The modal propagation constant β_x is found by substituting $\underline{e}_t = \tilde{\underline{e}}_t = \underline{e}_x$ into equation 2.12, while β_y is found by substituting $\underline{e}_t = \tilde{\underline{e}}_t = \underline{e}_y$ into equation 2.12. I have now fully specified the general characteristics of the fundamental modes on waveguides with a pair of preferred symmetry axes. The details depend upon knowing the solution of the scalar wave equation. The transmission properties of such waveguides, when propagating only the fundamental modes, are similar to these of anisotropic crystals, in that the waveguide has a pair of optical axes.[3]

2. The Higher Order Modes

In general, the higher order modal fields of structures with two preferred axes of symmetry are more complicated than those of the fundamental modes. In order to appreciate this complication, begin by considering the ellipse. It is clear that for a sufficiently large eccentricity the field of any particular mode is given by equation 2.7, so that the only difference between it and a fundamental mode is in ψ and β. However it is equally clear that for a sufficiently small eccentricity, this same mode resembles a modal field of a circularly symmetric waveguide, with $\hat{x}$ and $\hat{y}$ parallel to the symmetry axes of the ellipse. This transition is sketched in Figure 3.3. We can associate each ellipse mode with the fields of a distorted circle mode. For example, the ellipse mode that corresponds to distorting either $\underline{e}_{t1}$ or $\underline{e}_{t2}$ of Figure 3.1 is formed by a linear combination of $\tilde{\underline{e}}_{xe}$ and $\tilde{\underline{e}}_{yo}$, where these $\tilde{\underline{e}}$'s are now solutions to the scalar wave equation in elliptical geometry. Consequently, the fields of the ellipse modes $\underline{e}_{t1}$ and $\underline{e}_{t2}$ are

$$\underline{e}_{ti} = a^{i}_{ex}\psi_{e}\hat{\underline{x}} + a^{i}_{oy}\psi_{o}\hat{\underline{y}} \tag{3.7}$$

where i = 1 or 2, ψ_e and ψ_o are solutions of the scalar wave equation in elliptical geometry and are analogous to ψ_e and ψ_o given by equation 3.1 for the scalar wave equation in cylindrical geometry. Figure 3.4 provides an example of ψ_e and ψ_o. The propagation constants associated with ψ_e and ψ_o are denoted $\tilde{\beta}_e$ and $\tilde{\beta}_o$ respectively. The $\tilde{\beta}$'s are different, the difference increases as the eccentricity increases.

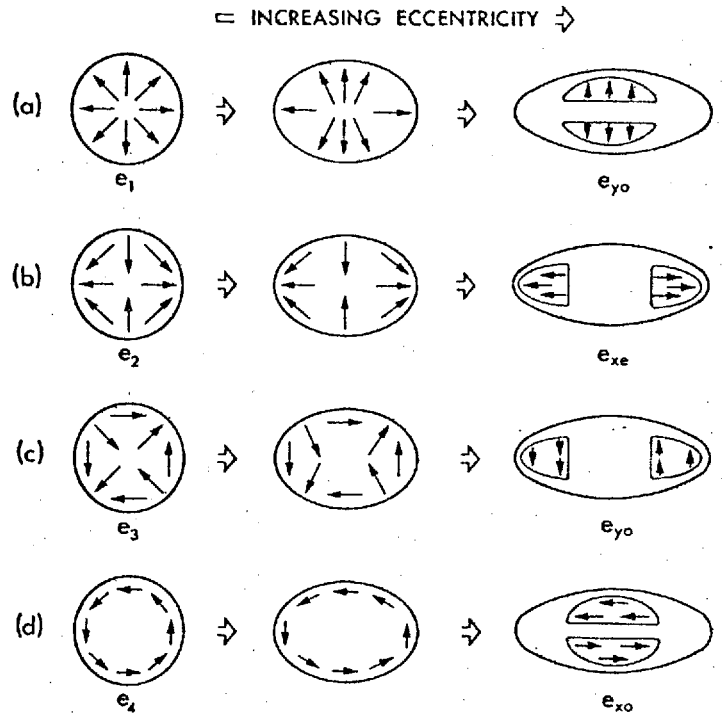

Figure 3.3: Transition from circle to ellipse modes for $\ell = 1$ modes. An electric field vector maintains its orientation to the interface, i.e., if it was initially perpendicular it remains perpendicular, as the eccentricity increases. Using this heuristic principle one can anticipate the way in which a particular circle mode changes as the eccentricity increases.

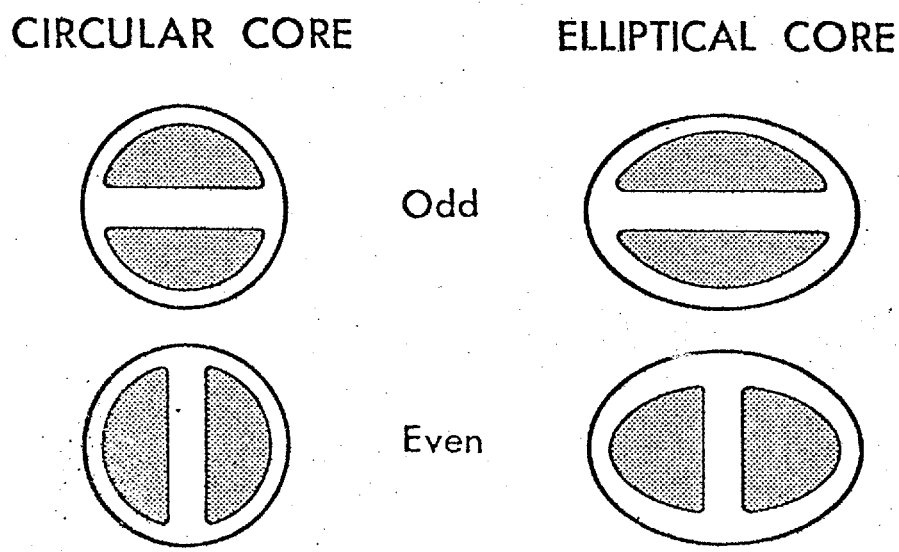

Figure 3.4: An example of a solution of the scalar wave equation corresponding to the $\ell = 1$ mode. The $\tilde{\beta}$'s of the even and odd circle mode are identical unlike the $\tilde{\beta}$'s for the even and odd modes of the elliptical core.

A heuristic argument can be used to determine the minimum eccentricity necessary for the $\ell \geq 1$ ellipse modes to be uniformly polarised, i.e., to have the form given by equation 3.6. Anticipating that only a slight eccentricity is necessary, the fields of the ellipse can be approximated by linear combinations of the circle $n_{co} = n_{c1}$ fields $\tilde{\underline{e}}_{xe}$, $\tilde{\underline{e}}_{yo}$ as far as the present discussion is concerned.

Now there are two small parameters which determine the composition of a mode, the eccentricity e and the critical angle θ_c. It is clear that as these two parameters go to zero they have competitive effects since:

a) When $e \neq 0$ and $\theta_c = 0$ the $n_{co} = n_{c1}$ or LP modes in equation 2.7 are the modes of the structure. The stability of linear combinations of these modes depends on $\tilde{\beta}_e - \tilde{\beta}_o$.

b) When $e = 0$ and $\theta_c \neq 0$ the circle modes in equation 3.5 are the modes of the structure. The stability of linear combinations of these modes depends on $\beta_{HE} - \beta_{EH}$ (see the discussion at the end of Section 3.1).

Consequently the parameter

$$\Lambda = (\tilde{\beta}_e - \tilde{\beta}_o)/(\beta_{EH} - \beta_{HE}) \tag{3.8}$$

is influential in determining the composition of the modes of a structure with $e \neq 0$ and $\theta_c \neq 0$. When $|\Lambda| >> 1$, the modes are LP or $n_{co} = n_{c1}$ modes. When $|\Lambda| << 1$, the modes are circle modes.

The argument above is tantamount to determining the limiting behavior of a^i_{ex}/a^i_{ox} of equation 3.7. An expression for this ratio can be found using the prescription outlined

in Section 2.2. The β of the ellipse vector modal field equation 3.7 is by substituting $\underline{e}_{tl}$ in equation 2.12 for $\underline{e}_t$ and substituting either $\tilde{\underline{e}}_{xe}$ or $\tilde{\underline{e}}_{yo}$ in equation 2.12 for $\tilde{\underline{e}}_t$. The fact that we have two expressions for the same β gives us two equations which determine the ratio a^i_{ex}/a^i_{oy} of equation 3.7 in addition to β_i. The algebra has been relegated to Appendix A. For small eccentricity

$$a^i_{ex}/a^i_{oy} = \Lambda \pm (\Lambda^2 + 1)^{1/2} \tag{3.9}$$

$$\beta_i^2 = \{(\tilde{\beta}_e^2 + \tilde{\beta}_o^2)/2\} \pm [\{(\tilde{\beta}_o^2 - \tilde{\beta}_e^2)/2\}^2 + C^2]^{1/2} \tag{3.10}$$

where i = 1 is associated with + while i = 2 is associated with -. The parameter C is

$$C = \int_{A_\infty} \tilde{\underline{e}}_{xe} \cdot \underline{\nabla}_t (\tilde{\underline{e}}_{yo} \cdot \underline{\nabla}_t \ell n \varepsilon) dA / \int_{A_\infty} |\tilde{\underline{e}}_{xe}|^2 \, dA \tag{3.11}$$

$$= \beta_{EH}^2 - \beta_{HE}^2 \cong 2k(\beta_{EH} - \beta_{HE}) \tag{3.12}$$

and Λ is

$$\Lambda = (\tilde{\beta}_e^2 - \tilde{\beta}_o^2)/2C \cong (\tilde{\beta}_e - \tilde{\beta}_o)/(\beta_1 - \beta_2) \tag{3.13}$$

which is the same as the intuitively derived equation 3.8. Thus, the composition of a mode depends only on the parameter Λ. When $\Lambda = 0$, the modes are essentially circle modes. When $\Lambda >> 1$ the modes are $n_{co} = n_{cl}$ modes. Equations 3.3 to 3.12 are for modes 1 and 2 of the ellipse, when $\ell \geq 1$. The remaining two ellipse modes are found analogously.

Identical arguments can be applied to all structures with two preferred axes of symmetry, e.g., the composite two waveguide system of Figure 3.2. Furthermore, the procedure can clearly be generalized to other waveguides.

Bibliography and Footnotes for Chapter 3

1. N.S. Kapany and J.J. Burke, Optical Waveguides, Academic Press, New York (1972).

2. D. Marcuse, Light Transmission Optics, Van Nostrand Reinhold, Princeton, New Jersey (1972).

3. M. Born and E. Wolf, Principles of Optics, 3rd edition, Pergamon Press, New York (1964).

4. Take the field $\tilde{\underline{e}}_{ex} = \cos\ell\phi\ \hat{x}$ for example. If one rotates the coordinates through an angle $-\alpha$, i.e.

$$\phi = \phi^1 + \alpha\ ,\ \hat{x} = \cos\alpha\hat{x}^1 - \sin\alpha\hat{y}^1$$

then the field in terms of the new coordinates is

$$\begin{aligned}\tilde{\underline{e}}_{ex} &= \cos^2\alpha\ \cos\ell\phi^1\ \hat{x}^1 - \sin\alpha\ \cos\alpha\ \cos\ell\phi^1\ \hat{y}^1 \\ &\quad - \sin\alpha\ \cos\alpha\ \sin\ell\phi^1\ \hat{x}^1 + \sin^2\alpha\ \sin\ell\phi^1\ \hat{y}^1 \\ &= \cos^2\alpha\ \tilde{\underline{e}}^1_{xe} - \sin\alpha\ \cos\alpha\ \tilde{\underline{e}}^1_{ye} \\ &\quad - \sin\alpha\ \cos\alpha\ \tilde{\underline{e}}^1_{xo} + \sin^2\alpha\ \tilde{\underline{e}}^1_{yo}\end{aligned}$$

i.e., a linear combination of all four $\tilde{\underline{e}}^1$. Of course, rotating the coordinates through an angle $-\alpha$ is equivalent to rotating the waveguide through an angle α.

CHAPTER 4

EXAMPLES: STEP REFRACTIVE INDEX WAVEGUIDES

Chapters 2 and 3 show how to construct the vector modal fields $\underline{e}$, $\underline{h}$ and their propagation constants β from linear combinations of solutions ψ to the scalar wave equation, equation 2.8. Thus, when ψ is known the modes are fully specified. I shall first determine the modes of a step profile with circular symmetry, since the results can then be compared with the exact forms.[1,2] Next, I consider a waveguide with an elliptic core and then a composite two parallel cylinder waveguide. These last two examples exhibit several interesting physical properties which the $n_{co} \cong n_{cl}$ method readily displays.

4.1 Step Index Waveguide with Circular Symmetry

The radial function $f_\ell(r)$ for a step profile is found from equation 3.2 and can be written as

$$f_\ell(r) = J_\ell(\tilde{U}r/\rho)/J_\ell(\tilde{U}) \qquad r \leq \rho \tag{4.1a}$$

$$f_\ell(r) = K_\ell(\tilde{W}r/\rho)/K_\ell(\tilde{W}) \qquad r \geq \rho \tag{4.1b}$$

where the notation $\tilde{}$ indicates a quantity derived from the scalar wave equation. Note that $\ell = 0$ is the fundamental mode, $\ell = 1$ the second mode set and so on. The requirement that $f_\ell(r)$ and $df_\ell(r)/dr$ be continuous at $r = \rho$ gives the eigenvalue equation

$$\tilde{U}\, J_{\ell+1}(\tilde{U}) K_\ell(\tilde{W}) = \tilde{W}\, K_{\ell+1}(\tilde{W}) J_\ell(\tilde{U}) \tag{4.2}$$

after using the well known recurrence relations for Bessel functions. $\tilde{U}$ and $\tilde{W}$ are related to the dimensionless parameter V defined by equation 2.3 as

$$\tilde{U}^2 + \tilde{W}^2 = V^2 \ . \tag{4.3}$$

The modal propagation constant $\tilde{\beta}$ is given by

$$(\rho\tilde{\beta})^2 = (\rho k_{co})^2 - \tilde{U}^2 = (\rho k_{cl})^2 + \tilde{W}^2 \ . \tag{4.4}$$

The modal vector fields can then be formed as discussed in Section 3 and are listed in Table 4.1. The propagation constants β are found by substituting the expressions for $\underline{e}_t$ in Table 4.1 into equation 2.12 for $\underline{e}_t$ and substituting either of the two $\underline{\tilde{e}}$ fields used to form $\underline{e}_t$ into equation 2.12 for $\underline{\tilde{e}}_t$. All the integrals are elementary or have been calculated elsewhere[3] and included in Table 4.1. The corrections to $\tilde{\beta}$ are also listed in Table 4.1. The corrections to $\tilde{\beta}$ obtained using the $n_{co} \cong n_{cl}$ method agree with the corrections obtained from the exact eigenvalue equation, see Appendix B. The present approach streamlines the original derivation[3] and in addition provides simple analytic expressions for improving $\tilde{\beta}$ by including the effects of the $\nabla_t \ell n \varepsilon$ term in the vector wave equation. Discarding terms of order θ_c^2 from the exact expression for $\underline{e}_t$, terms of order θ_c^3 for e_z and terms of order θ_c^5 for β leads to the results in Table 4.1.

Finally, because the step profile is the most rapidly varying $\varepsilon(x,y)$ possible, it is therefore the most sensitive to polarisation effects, i.e., most sensitive to the $\nabla_t \ell n \varepsilon$

TABLE 4.1

	Mode 1, $EH_{\ell-1}$ odd	Mode 2, $HE_{\ell+1}$ even	Mode 3, $HE_{\ell+1}$ odd	Mode 4, $EH_{\ell-1}$ even
	$\underline{e}_1 = \underline{\tilde{e}}_{ex} + \underline{\tilde{e}}_{oy}$	$\underline{e}_2 = \underline{\tilde{e}}_{ex} - \underline{\tilde{e}}_{oy}$	$\underline{e}_3 = \underline{\tilde{e}}_{ox} + \underline{\tilde{e}}_{ey}$	$\underline{e}_4 = \underline{\tilde{e}}_{ox} - \underline{\tilde{e}}_{ey}$
Transverse electric field, $\underline{e}_t$ $f_\ell(r) = \begin{cases} J_\ell(\tilde{U}r/\rho)/J_\ell(\tilde{U}) & r<\rho \\ K_\ell(\tilde{W}r/\rho)/K_\ell(\tilde{W}) & r>\rho \end{cases}$	$(\cos\ell\phi\,\hat{x} + \sin\ell\phi\,\hat{y})f_\ell(r)$ $= (\cos(\ell-1)\phi\,\hat{r} + \sin(\ell-1)\phi\,\hat{\phi})f_\ell(r)$	$(\cos\ell\phi\,\hat{x} - \sin\ell\phi\,\hat{y})f_\ell(r)$ $= (\cos(\ell+1)\phi\,\hat{r} - \sin(\ell+1)\phi\,\hat{\phi})f_\ell(r)$	$(\sin\ell\phi\,\hat{x} + \cos\ell\phi\,\hat{y})f_\ell(r)$ $= (\sin(\ell+1)\phi\,\hat{r} + \cos(\ell+1)\phi\,\hat{\phi})f_\ell(r)$	$(\sin\ell\phi\,\hat{x} - \cos\ell\phi\,\hat{y})f_\ell(r)$ $= (\sin(\ell-1)\phi\,\hat{r} - \cos(\ell-1)\phi\,\hat{\phi})f_\ell(r)$
Longitudinal Electric Field $g_\ell^{\pm}(r) = \begin{cases} J_{\ell\pm1}(\tilde{U}r/\rho)/J_\ell(\tilde{U}) & r<\rho \\ K_{\ell\pm1}(\tilde{W}r/\rho)/K_\ell(\tilde{W}) & r>\rho \end{cases}$	$-i\frac{\tilde{U}}{V}\theta_c\, g_\ell^-(r)\cos(\ell-1)\phi$	$i\frac{\tilde{U}}{V}\theta_c\, g_\ell^+(r)\cos(\ell+1)\phi$	$i\frac{\tilde{U}}{V}\theta_c\, g_\ell^+(r)\sin(\ell+1)\phi$	$-i\frac{\tilde{U}}{V}\theta_c\, g_\ell^-(r)\sin(\ell-1)\phi$
Modal Power $P = \frac{1}{2}\int_{A_\infty} \underline{e}_t \times \underline{h}_t^* \cdot \hat{z}\, dA$ $= \frac{1}{2}\sqrt{\frac{\varepsilon_{co}}{\mu}}\int_{A_\infty} \lvert\underline{e}_t\rvert^2 dA$	$P = \frac{1}{2}\pi\rho^2\sqrt{\frac{\varepsilon_{co}}{\mu}}\left(\frac{V}{\tilde{U}}\right)^2 \xi_\ell$ where $\xi_\ell = \frac{K_{\ell+1}(\tilde{W})\,K_{\ell-1}(\tilde{W})}{K_\ell^2(\tilde{W})}$			
Propagation Constant β $\tilde{\beta} = \{k_{co}^2 - (\tilde{U}/\rho)^2\}^{1/2}$ $\beta - \tilde{\beta} = \frac{\int_{A_\infty} \underline{e}_t \cdot \nabla_t(\underline{e}_t \cdot \nabla_t \ln\varepsilon)\, dA}{2k_{co}\int_{A_\infty}\lvert\underline{e}_t\rvert^2 dA}$	$\beta-\tilde{\beta} = -\frac{\theta_c^3}{4\rho}\frac{\tilde{U}^2\tilde{W}}{V^3}\frac{K_{\ell-1}(\tilde{W})}{K_\ell(\tilde{W})}$ if $\ell \neq 1$ $\beta-\tilde{\beta} = -\frac{\theta_c^3}{2\rho}\frac{\tilde{U}^2\tilde{W}}{V^3}\frac{K_0(\tilde{W})}{K_1(\tilde{W})}$ if $\ell = 1$	$\beta-\tilde{\beta} = -\frac{\theta_c^3}{4\rho}\frac{\tilde{U}^2\tilde{W}}{V^3}\frac{K_\ell(\tilde{W})}{K_{\ell-1}(\tilde{W})}$ for all ℓ	$\beta-\tilde{\beta} = -\frac{\theta_c^3}{4\rho}\frac{\tilde{U}^2\tilde{W}}{V^3}\frac{K_\ell(\tilde{W})}{K_{\ell-1}(\tilde{W})}$ for all ℓ	$\beta-\tilde{\beta} = -\frac{\theta_c^3}{4\rho}\frac{\tilde{U}^2\tilde{W}}{V^3}\frac{K_{\ell-1}(\tilde{W})}{K_\ell(\tilde{W})}$ if $\ell \neq 1$ $\beta-\tilde{\beta} = 0$ if $\ell = 1$

term in the vector wave equation. Thus the step profile provides a stringent test of the $n_{co} \cong n_{cl}$ method.

4.2 Stability of the LP or $n_{co} = n_{cl}$ Modes

The $n_{co} = n_{cl}$ or LP modes are not modes of an $n_{co} \cong n_{cl}$ waveguide. Each LP mode is formed by combining two proper modes, an $HE_{\ell+1,m}$ and $EH_{\ell-1,m}$ mode. These proper modes have different propagation constants, β_{HE} and β_{EH}. Because of the beat phenomenon, when $\beta_{HE} \neq \beta_{EH}$, the LP modes rotate or fade into each other,[4] e.g., $\underline{\tilde{e}}_{xe}$ of Figure 3.1 after propagating a distance $\pi/|\beta_{HE}-\beta_{EH}|$, which equals half the beat length, rotates into $\underline{\tilde{e}}_{yo}$ of Figure 3.1. The greater $|\beta_{HE}-\beta_{EH}|$, the shorter the beat length and hence the more rapidly the LP modes rotate. From Table 4.1 when $\ell = 1$

$$\beta_{TM}-\beta_{HE} = \theta_c^3\tilde{U}^2K_1^2(\tilde{W})\{2-(\tilde{W}K_o(\tilde{W})/K_1(\tilde{W}))\}/2\rho V^3K_o(\tilde{W})K_2(\tilde{W}) \qquad (4.5a)$$

$$\beta_{TE}-\beta_{HE} = \theta_c^3\tilde{U}^2K_1^2(\tilde{W})\{2+(\tilde{W}K_o(\tilde{W})/K_1(\tilde{W}))\}/2\rho V^3K_o(\tilde{W})K_2(\tilde{W}) \qquad (4.5b)$$

and when $\ell \geq 2$

$$\beta_{EH}-\beta_{HE} = \ell\theta_c^3\tilde{U}^2K_\ell^2(\tilde{W})/\rho V^3K_{\ell-1}(\tilde{W})K_{\ell+1}(\tilde{W}) \qquad (4.6)$$

(recall that the 4 $\ell \geq 2$ modes occur in two degenerate pairs, the EH and HE pairs). The results for $\ell = 1$ are shown in Figure 4.1. Note the special characteristic that at $V \cong 3.8$ the $\underline{\tilde{e}}_{xe}$ and $\underline{\tilde{e}}_{yo}$ LP modes are true modes of the $n_{co} \cong n_{cl}$ waveguide because $\beta_{HE} = \beta_{TM}$ at this frequency. In contrast, at $V \cong 3.8$ $\beta_{TE} - \beta_{HE} \cong 0.25\ \theta_c^3/\rho$ corresponding to a

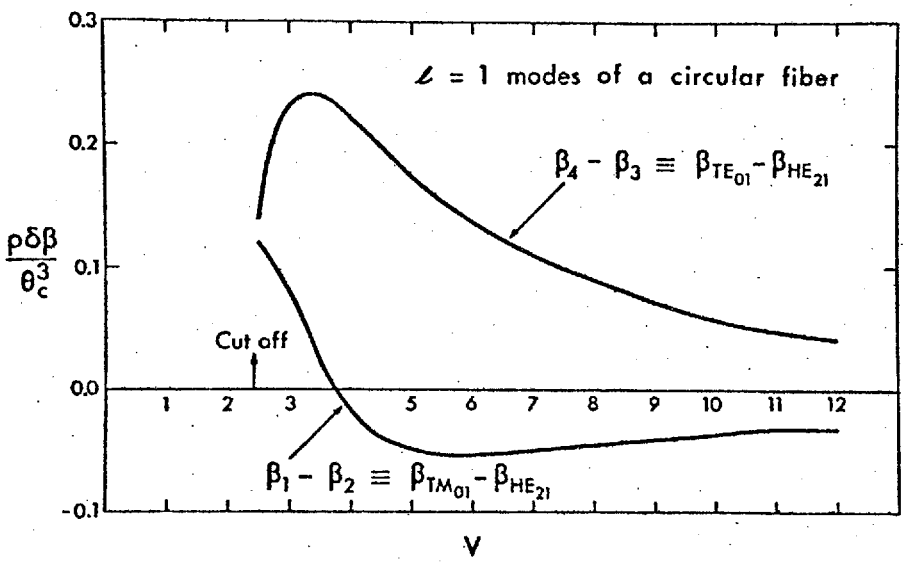

Figure 4.1: The difference in β's for $\ell = 1$ modes of the circularly symmetric, step profile waveguide. Each LP mode of Figure 3.1(a) is formed by linear combination of β_1, β_2 modes or β_3, β_4 modes.

half beat length of $1.3 \times 10^4 \rho$ for a typical value of $\theta_c = .1$. Thus near $V = 3.8$, the mode patterns $\underline{\tilde{e}}_{xe}$ and $\underline{\tilde{e}}_{yo}$ should appear stable compared to the other two patterns $\underline{\tilde{e}}_{xo}$ and $\underline{\tilde{e}}_{ye}$. When $V >> 1$, $|\beta_{TE}-\beta_{HE}| = |\beta_{TM}-\beta_{HE}| \cong \theta_c^3 \tilde{U}^2/\rho V^2$.

From equation 4.6, the β's are never equal for $\ell \geq 2$, so the $\ell \geq 2$ LP modes are never modes of the circularly symmetric waveguide. Futhermore, the greater ℓ, the greater $|\beta_{HE}-\beta_{EH}|$, which approximately equals $\theta_c^3 \ell \tilde{U}^2/2\rho V^3$ for $\ell >> 1$. Consequently for fixed V, the greater ℓ the less stable the LP modes.

4.3 The Step Index Ellipse

The consequences of an elliptic deformation of a circular waveguide are sketched in Figure 3.3. As the eccentricity increases the ellipse modes become uniformly polarised, i.e., $\underline{e}$ is parallel to one of the two symmetry axes. It is interesting to determine the minimum eccentricity required for the $n_{co} = n_{cl}$ or LP modes of Figure 3.1 to be the proper ellipse modes.[6] On a waveguide with this minimum eccentricity, the modes of a circularly symmetric waveguide are unstable, i.e., they couple power among themselves as they propagate, while the $n_{co} = n_{cl}$ modes are stable. It was shown in Section 3.2(2) that the composition of the proper modes depends crucially on

$$\Lambda = (\tilde{\beta}_e - \tilde{\beta}_o)/(\beta_{EH} - \beta_{HE}) \qquad (4.7)$$

where β_{EH}, β_{HE} are the propagation constants for the two mode types on a circular waveguide[6] (Sections 4.1 and 4.2)

while $\tilde{\beta}_e$ and $\tilde{\beta}_o$ are the propagation constants of the even and odd solutions of the scalar wave equation in elliptical geometry. When $\Lambda >> 1$, the modal fields are LP fields while when $\Lambda << 1$ the modal fields are circle fields.

1. $\ell = 1$ Ellipse Modes

The quantity $\beta_{EH}-\beta_{HE}$ in equation 4.7 has been stated in equations 4.5 and 4.6.[6] When the eccentricity is small $\tilde{\beta}_e-\tilde{\beta}_o$ is determined from the scalar wave equation in circular geometry using the scalar perturbation theory in Chapter 5 (see Section 5.2(2)), leading to

$$\tilde{\beta}_e-\tilde{\beta}_o = \theta_c e^2 \tilde{U}^2 K_1^2(\tilde{W})/4\rho V K_o(\tilde{W}) K_2(\tilde{W}) \qquad (4.8)$$

where $\tilde{U}$ and $\tilde{W}$ are found from equations 4.2 and 4.3 and e is the eccentricity of the waveguide. Consequently for $\ell = 1$, Λ in equation 4.7 is

$$\Lambda = e^2V^2/2\theta_c^2\{2 \pm (\tilde{W}K_o(\tilde{W})/K_1(\tilde{W}))\} \qquad (4.9)$$

where the negative sign is for Λ_{TM}, i.e., for $\beta_{EH}-\beta_{HE}$ in equation 4.7 to be $\beta_{TM}-\beta_{HE}$ while the positive sign applies to Λ_{TE}, i.e., for $\beta_{TE}-\beta_{HE}$ in equation 4.7. Equation 4.9 exhibits the sensitivity of Λ to eccentricity, e, defined in Figure 3.2, and the refractive index difference, defined by equation 1.12. If V is fixed, the smaller θ_c, the less eccentricity is required for the LP modes of the circular cylinder to be stable modes of the ellipse. Figure 4.2 provides a graph of $(\theta_c/e)^2\Lambda$ vs. V. Remembering that when $\Lambda >> 1$, the LP modes are the modes of the ellipse while when

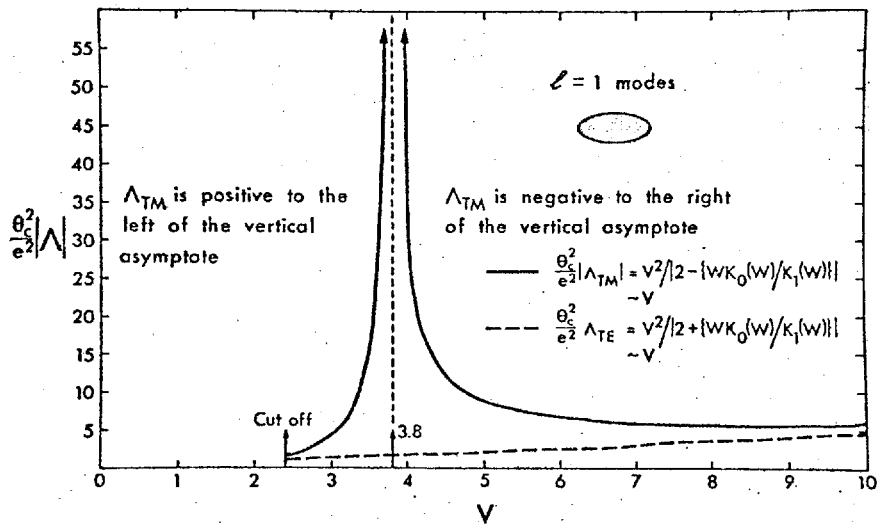

Figure 4.2: The parameter Λ defined by equation (4.9) determines the ratio a_i/b_i of the ellipse $\ell = 1$ fields, equation (3.9). When $|\Lambda| >> 1$, the modes are uniformly polarized (LP modes) while when $|\Lambda| << 1$ the modal fields are those of a circular core.

$\Lambda << 1$ the linear combinations in equation 3.5 are modes of the ellipse, we see that no eccentricity is required for the LP modes $\tilde{\underline{e}}_{xe}$ and $\tilde{\underline{e}}_{yo}$ to be ellipse modes at $V \cong 3.8$. This is anticipated from Figure 4.1, since at $V \cong 3.8$, $\beta_{TM} = \beta_{HE}$, i.e., the LP modes $\tilde{\underline{e}}_{xe}$ and $\tilde{\underline{e}}_{yo}$ are true modes of the circular cylinder without any perturbation. Since even the minimum value for $\Lambda \cong 2(e/\theta_c)^2$, only a minute eccentricity ($e \geq 2\theta_c$) is required for the LP modes to be stable. The stability of the higher order ellipse modes can be investigated in a similar fashion. In general the compositions of the higher order circle modes are much less sensitive to small elliptic deformations of the core.

2. Fundamental or $\ell = 0$ Ellipse Modes

In Section 3.2(1) it was noted that the transmission properties of an elliptical waveguide propagating only the two fundamental modes are similar to those of an anisotripic crystal, i.e., both structures have orthogonal optical axes. The optical properties of the waveguide depend on the difference in propagation constants β_x, β_y of the x and y polarised ellipse modes. This difference can be found by substituting the fields $\tilde{\underline{e}}_x = \psi\hat{x}$ and $\tilde{\underline{e}}_y = \psi\hat{y}$ into equation 2.12 to determine β_x and β_y, where ψ is a solution to the scalar wave equation in elliptical geometry. It is not sufficient to approximate ψ by solutions of the scalar wave equation in circular geometry as was done in Section 4.3(1). Instead higher order terms in an expansion in powers of eccentricity are necessary. Alternatively, one can use the second perturbation method in Chapter 5 (see Sections 5.3, 5.4) and perturb about Maxwell's equations in circular geometry.

The result obtained there is

$$\beta_x - \beta_y = e^2 \theta_c^3 \tilde{U}^2 \tilde{W}^2 \{1 + (\tilde{U} K_o^2(\tilde{W}) J_2(\tilde{U}) / K_1^2(\tilde{W}) J_1(\tilde{U}))\} / 8\rho V^3 \qquad (4.10)$$

assuming $e^2 << 1$ and $\theta_c^2 << 1$. In equation 4.10 $\tilde{U}$ and $\tilde{W}$ are found from equations 4.2 and 4.3 for $\ell = 0$. If the fiber is illuminated by linearly polarised light at 45° to the optical or symmetry axes, then both fundamental modes are equally excited and the guided wave is elliptically polarised. Because of the beat phenomenon the $\underline{E}$ vector rotates. The length for a 360° rotation is $2\pi/|\beta_x - \beta_y|$. In Figure 4.3 $\beta_x - \beta_y$ vs. V from equation 4.10 has been plotted.

4.4 Two Identical Parallel Step Index Waveguides

The determination of the modes of the composite two waveguide system of Figure 3.2 is completely analogous to that of the ellipse as outlined in Section 3.2(2), except that the scalar solution ψ for the two cylinder geometry is required. There is no exact solution for ψ. Instead ψ is approximated, in the usual manner, by a symmetric and antisymmetric superposition of the fields of the waveguides in isolation. The scalar propagation constant $\tilde{\beta}$ is approximated using the same perturbation method on the scalar wave equation as with the ellipse (see Chapter 5).

The scalar wave equation appropriate to the present problem is

$$\{\nabla_t^2 + k^2\}\psi = \tilde{\beta}^2 \psi \qquad (4.11)$$

where

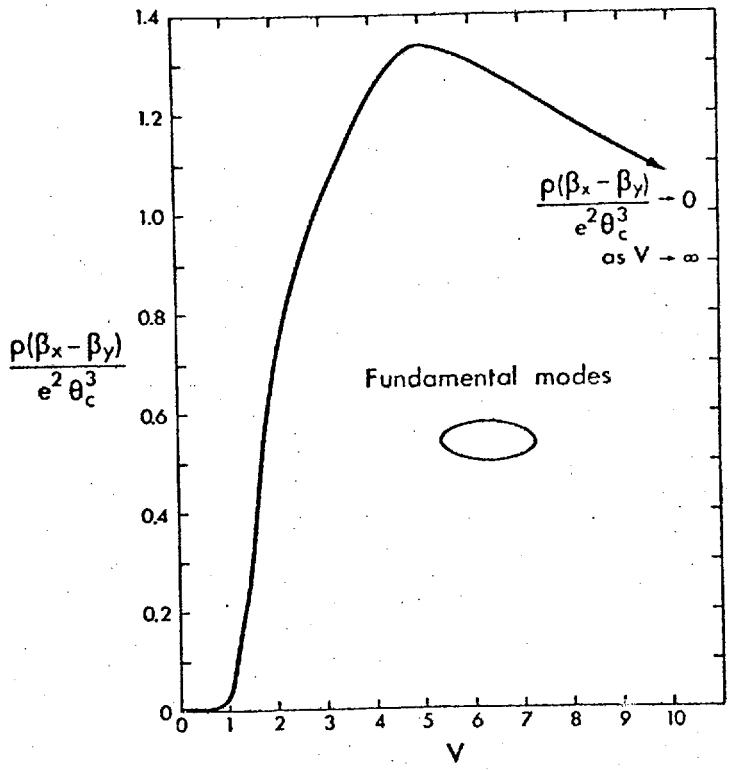

Figure 4.3: The difference in β's of the x and y polarized, fundamental ellipse modes.

$$k = \begin{cases} k_{co} \text{ in the cores of the fibers} \\ k_{cl} \text{ elsewhere} \end{cases} \tag{4.12}$$

The approximate solutions of equation 4.11 used in this section are

$$\psi_{\pm} = \psi_1 \pm \psi_2 \tag{4.13}$$

where ψ_1 is a scalar mode of fiber 1 in isolation and ψ_2 is the corresponding scalar mode of fiber 2 in isolation. The scalar modes ψ_1 and ψ_2 satisfy the scalar wave equations

$$\{\nabla_t^2 + k_{1,2}^2\}\psi_{1,2} = \tilde{\tilde{\beta}}^2\psi_{1,2} \tag{4.14}$$

where k_1 and k_2 are the local wavenumbers of the isolated fibers 1 and 2 respectively.

The propagation constant, $\tilde{\tilde{\beta}}$ in equation 4.14, is an approximation of $\tilde{\beta}$ in equation 4.11. This approximation is improved using the scalar perturbation theory of Chapter 5. The results for the fundamental mode (i.e., $\psi_1 = f_o(r_1)$ and $\psi_2 = f_o(r_2)$ are

$$\tilde{\beta}_+^2 = \tilde{\tilde{\beta}}^2 + 2\tilde{U}^2K_o(\tilde{W}d/\rho)/\rho^2V^2K_1^2(\tilde{W}) \tag{4.15a}$$

$$\tilde{\beta}_-^2 = \tilde{\tilde{\beta}}^2 - 2\tilde{U}^2K_o(\tilde{W}d/\rho)/\rho^2V^2K_1^2(\tilde{W}) \quad . \tag{4.15b}$$

1. The Fundamental Modes

Once the scalar wave equation has been solved, one constructs approximations of the electric fields of the four

fundamental modes viz

$$\underline{e}_{x+} = \psi_+ \, \hat{\underline{x}} \tag{4.16a}$$

$$\underline{e}_{x-} = \psi_- \, \hat{\underline{x}} \tag{4.16b}$$

$$\underline{e}_{y+} = \psi_+ \, \hat{\underline{y}} \tag{4.16c}$$

$$\underline{e}_{y-} = \psi_- \, \hat{\underline{y}} \, . \tag{4.17d}$$

The electric fields of the four fundamental modes are sketched in Figure 4.4; each mode has a different β and an electric field parallel to one of the two axes of symmetry (see Section 3.2(1)).

Equations 4.16 are now substituted into equation 2.12 to correct the model propagation constants for polarisation effects. The details of the algebra are collected in Appendix C; the final results are:

$$\beta_{x+}^2 = \tilde{\beta}_+^2 + \theta_c^2/\rho^2(\tilde{U}/V)^2[\tilde{W}K_o(\tilde{W})/K_1(\tilde{W}) + \{1 - 2I_1(\tilde{W})K_1(\tilde{W})\} \cdot K_o(d/\rho\tilde{W})/K_1^2(\tilde{W})] \tag{4.18a}$$

$$\beta_{x-}^2 = \tilde{\beta}_-^2 + \theta_c^2/\rho^2(\tilde{U}/V)^2[\tilde{W}K_o(\tilde{W})/K_1(\tilde{W}) + \{1 - 2I_1(\tilde{W})K_1(\tilde{W})\} \cdot K_o(d/\rho\tilde{W})/K_1^2(\tilde{W})] \tag{4.18b}$$

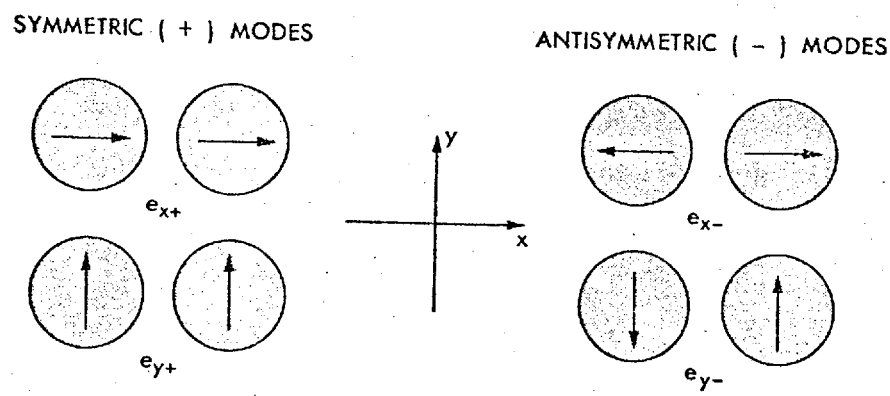

Figure 4.4: The 4 fundamental modes of the two parallel waveguide system shown in Figure 3.2 .

$$\beta_{y+}^2 = \tilde{\beta}_+^2 + \theta_c^2/\rho^2(\tilde{U}/V)^2[\tilde{W}K_o(\tilde{W})/K_1(\tilde{W})$$

$$- \{1 - 2I_1(\tilde{W})K_1(\tilde{W})\} \cdot K_o(d/\rho\tilde{W})/K_1^2(\tilde{W})] \qquad (4.18c)$$

$$\beta_{y-}^2 = \tilde{\beta}_-^2 + \theta_c^2/\rho^2(\tilde{U}/V)^2[\tilde{W}K_o(\tilde{W})/K_1(\tilde{W})$$

$$- \{1 - 2I_1(\tilde{W})K_1(\tilde{W})\} \cdot K_o(d/\rho\tilde{W})/K_1^2(\tilde{W})] \qquad (4.18d)$$

where $\tilde{\beta}_+^2$ and $\tilde{\beta}_-^2$ are given by equation 4.15. Note how the inclusion of the effects of the polarisation term ensures that all four modes have different β's.

The difference between β_{x+} and β_{x-} (which equals $\beta_{y+} - \beta_{y-}$) gives rise to the familiar phenomenon of power transfer between parallel fibers.[1,5] For example, suppose that initially the field on the waveguide is

$$\underline{e}_{+x} - \underline{e}_{-x} = \psi_1 \hat{x} \qquad (4.19)$$

so that, in effect, the fundamental mode of fiber 1 in isolation has been excited. Since $\beta_{+x} \neq \beta_{-x}$, the modes present in the initial field beat. The beat length (i.e., the length in which all the power is transferred from fiber 1 to fiber 2 and back again) is

$$L_{trans} = 2\pi/|\beta_{+x} - \beta_{-x}| \qquad (4.20a)$$

$$= \pi\rho V^3 K_1^2(\tilde{W})/\theta_c \tilde{U}^2 K_o(\tilde{W}d/\rho) \ . \qquad (4.20b)$$

The difference between β_{x+} and β_{y+} (which equals $\beta_{x-}-\beta_{y-}$) can produce a rotation of the electric field of the waveguide. For example, suppose that initially the field on the waveguide is

$$\underline{e}_{x+} + \underline{e}_{y+} = (\psi_1 + \psi_2)(\hat{\underline{x}} + \hat{\underline{Y}}). \tag{4.21}$$

The beating of the modes produces a rotation of the electric field vector. The beat length in this case (i.e., the length in which the electric field rotates 2π) is

$$L_{rot} = 2\rho/|\beta_{x+}-\beta_{y+}| \tag{4.22a}$$

$$= 2\pi\rho V^2 K_1^2(\tilde{W})/\theta_c^3 \tilde{U}^2 K_o(\tilde{W}d/\rho)\{1-2I_1(\tilde{W})K_1(\tilde{W})\}. \tag{4.22b}$$

It is interesting to determine the angle $\alpha°$ that $\underline{E}$ rotates in the length necessary for total power transfer between the cylinders. This angle is 180° times L_{rot}/L_{trans}:

$$\alpha° = \theta_c^2\{1 - 2I_1(\tilde{W})K_1(\tilde{W})\}90° . \tag{4.23}$$

At $V = 2$ and $\theta_c = 0.1$, $\underline{E}$ rotates by 0.36° from its initial orientation of 45° to the symmetry axis in one exchange length.

2. The Higher Order Modes

From the four $\ell = 1$ modes of an isolated waveguide one can form eight symmetric and antisymmetric combinations, i.e., immediately above the four fundamental modes of the parallel waveguide system there are eight higher order modes.

The dependence of the higher order modes on the center to center separation d is directly analogous to the dependence of the ellipse modes on eccentricity. When the fibers are close, the modes of the two fiber system are well approximated by the $n_{co} = n_{cl}$ fields, i.e., by symmetric and antisymmetric combinations of the LP or $n_{co} = n_{cl}$ modes of each fiber in isolation, but with $\underline{E}$ parallel to the axes of symmetry. When the fibers are sufficiently separated, the modes are approximated by symmetric and antisymmetric combinations of the $n_{co} \cong n_{cl}$ modes of each fiber in isolation. An example is sketched in Figure 4.5. In other words, large eccentricity is analogous to small separation distance between the cylinders. The modes of the two waveguide system are formed by a linear combination of the same modes as for the ellipse. Accordingly, the logic of Section 3.2(2) applies directly. The parameter Λ is again important in establishing the limiting behaviour of the modal fields. As in the ellipse, the parameter Λ determines the composition of the modes.

Consider, for example, the symmetric solutions of the scalar wave equation

$$\psi_{+e} = f_1(r_1)\cos\phi_1 + f_1(r_2)\cos\phi_2 \qquad (4.24a)$$

$$\psi_{+o} = f_1(r_1)\sin\phi_1 + f_1(r_2)\sin\phi_2 \qquad (4.24b)$$

where

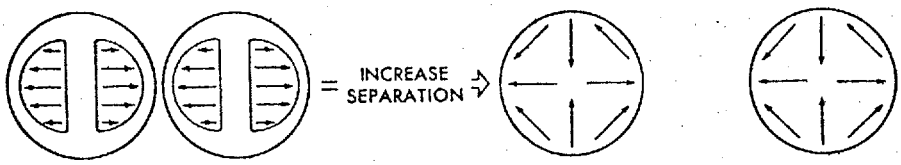

Figure 4.5: The transition of an $\ell = 1$ mode of the two parallel waveguide system as the separation increases. When the fibers are close, the composite mode appears like a superposition of two $\underline{\tilde{e}}_{xe}$ modes of Figure 3.1(a). When the fibers are well separated, the composite mode appears like a superposition of the $\underline{e}_2$ mode of Figure 3.1(b).

$$f_1(r) = \begin{cases} J_1(\tilde{U}r/\rho)/J_1(\tilde{U}) & r/\rho < 1 \\ K_1(\tilde{W}r/\rho)/K_1(\tilde{W}) & r/\rho > 1 \end{cases} \tag{4.25}$$

The $\tilde{\beta}$'s of the fields in equations 4.24 are (see Section 5.2(3))

$$\tilde{\beta}_{+e}^2 = \tilde{\tilde{\beta}}^2 + \tilde{U}^2\{K_1(\tilde{W}d/\rho) + K_2(\tilde{W}d/\rho)\}/\rho^2V^2K_o(\tilde{W})K_2(\tilde{W}) \tag{4.26a}$$

$$\tilde{\beta}_{+o}^2 = \tilde{\tilde{\beta}}^2 + \tilde{U}^2\{K_o(\tilde{W}d/\rho) - K_2(\tilde{W}d/\rho)\}/\rho^2V^2K_o(\tilde{W})K_2(\tilde{W}) \tag{4.26b}$$

where $\tilde{\tilde{\beta}}$ is defined in analogy with $\tilde{\beta}$ in equations 4.14, 4.15.

Now that the scalar equation has been solved we construct the $n_{co} = n_{cl}$ fields

$$\underline{\tilde{e}}_{+ex} = \psi_{+e}\,\hat{\underline{x}} \tag{4.27a}$$

$$\underline{\tilde{e}}_{+ey} = \psi_{+e}\,\hat{\underline{y}} \tag{4.27b}$$

$$\underline{\tilde{e}}_{+ox} = \psi_{+o}\,\hat{\underline{x}} \tag{4.27c}$$

$$\underline{\tilde{e}}_{+oy} = \psi_{+o}\,\hat{\underline{y}} \tag{4.27d}$$

(there are four more $n_{co} = n_{cl}$ fields formed from the antisymmetric solutions of the scalar wave equation). The $n_{co} = n_{cl}$ fields are linearly combined to approximate the $n_{co} \cong n_{cl}$ fields, e.g., the linear combination

$$\underline{e} = a_{+ex}\underline{\tilde{e}}_{+ex} + a_{+oy}\underline{\tilde{e}}_{+oy} \tag{4.28}$$

is motivated by the transition sketched in Figure 4.4. The parameter Λ in the equations analogous to equations 3.8 and 3.9 is

$$\Lambda = (\tilde{\beta}_{+e} - \tilde{\beta}_{+o})/(\beta_{EH} - \beta_{HE}) \tag{4.29}$$

$$= 2K_2(\tilde{W}d/\rho)/\theta_c^2 K_1^2(\tilde{W})\{2 \pm (\tilde{W}K_o(\tilde{W})/K_1(\tilde{W}))\} \; . \tag{4.30}$$

The negative sign in equation 4.30 applies for $\beta_{EH}-\beta_{HE} = \beta_{TM}-\beta_{HE}$, which is shown in Figure 4.6, while the positive sign is for $\beta_{TE}-\beta_{HE}$. When $\Lambda << 1$, the modes of the two cylinder waveguide are approximated by a mode of the circularly symmetric waveguide on each of the two cylinders. When $\Lambda >> 1$, the modes of the two cylinder waveguide are approximated by an $n_{co} = n_{cl}$ or LP mode on each of the two cylinders. Note that $\Lambda << 1$ when the two cylinders are well electromagnetically separated, i.e., when $d > 5\rho$ or when $V >> 1$. On the other hand, $\Lambda >> 1$ when the cylinders are electromagnetically close, i.e., when $d = 2\rho$ or $V \cong 2.4$.

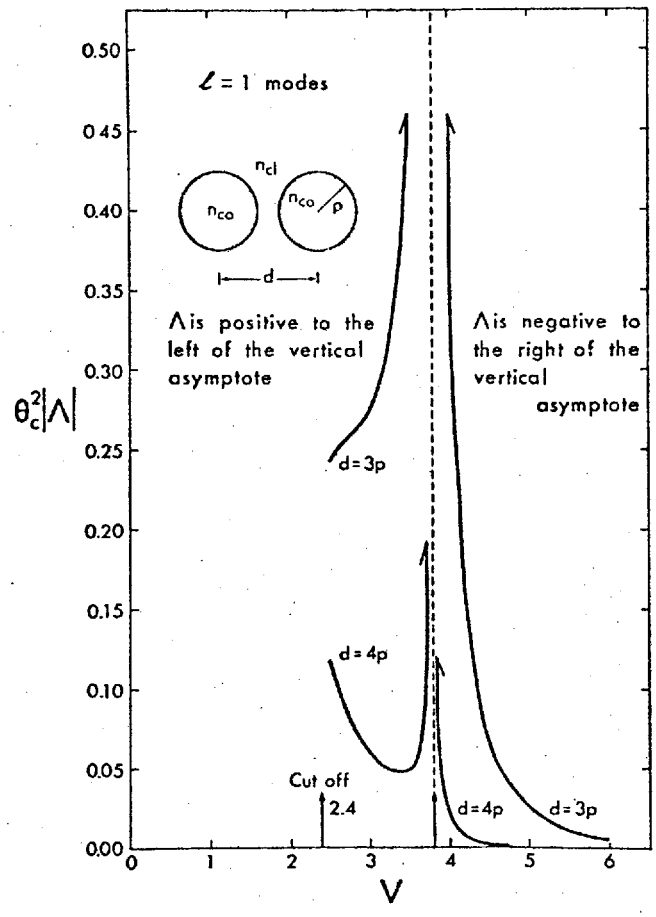

Figure 4.6: The parameter Λ defined by equation (4.30) which determines the composition of $\ell = 1$ modes.

Bibliography and Footnotes for Chapter 4

1. N.S. Kapany and J.J. Burke, Optical Waveguides, Academic Press, New York (1972).

2. D. Marcuse, Light Transmission Optics, Van Nostrand Reinhold, Princeton, New Jersey (1972).

3. A.W. Snyder, "Asymptotic expressions for eigenfunctions and eigenvalues of dielectric or optical waveguides," IEEE trans. MTT 17, 1130-1138 (1969).

4. E. Snitzer and H. Osterberg, "Observed dielectric waveguide modes in the visual spectrum," J. Opt. Soc. Am. 51, 499-505 (1961).

5. A.W. Snyder, "Coupled mode theory for optical fibers," J. Opt. Soc. Am. 62, 1268-1277 (1972).

6. We shall ultimately see that when $\theta_c << 1$, this minimum eccentricity is very small; despite this the perturbation method of this chapter is based on small θ_c, not small eccentricity. However, small eccentricity is used to simplify some of the intermediate steps in the application of the $n_{co} \cong n_{cl}$ method. In particular, Λ is evaluated approximately using the solution of the circular scalar wave equation.

CHAPTER 5

TWO PERTURBATION THEORIES

In this chapter I present two related perturbation theories. Both theories are derived by a deviation of the usual method used to prove orthogonality of solutions of a Sturm-Liouville equation.

5.1 Scalar Perturbation Theory

Solving the scalar wave equation is an important part of the $n_{co} \cong n_{cl}$ method. It is useful to be able to use known solutions of a scalar wave equation to approximate solutions of a scalar wave equation which cannot be solved exactly. This has been done in an ad hoc fashion in Sections 4.3 and 4.4. In this chapter I present a systematic approach to the problem.

Suppose one has two different scalar wave equations

$$\{\nabla_t^2 + k^2\}\psi = \tilde{\beta}^2\psi \tag{5.1a}$$

and

$$\{\nabla_t^2 + \bar{k}^2\}\bar{\psi} = \bar{\tilde{\beta}}^2\bar{\psi} \tag{5.1b}$$

(the $\tilde{}$ indicates a β associated with a scalar wave equation). Multiply equation 5.1a by $\bar{\psi}$ and equation 5.1b by ψ and subtract,

$$\{\bar{\psi}\nabla_t^2\psi - \psi\nabla_t^2\bar{\psi}\} + \{k^2 - \bar{k}^2\}\psi\bar{\psi} = \{\tilde{\beta}^2 - \bar{\tilde{\beta}}^2\}\psi\bar{\psi} \ . \tag{5.2}$$

Equation 5.2 is now integrated over the whole plane; Green's theorem is used to convert the first term to a line integral

at infinity, which is zero. The final result is

$$\tilde{\beta}^2 - \bar{\tilde{\beta}}^2 = \int_{A_\infty} (k^2-\bar{k}^2)\,\psi\bar{\psi}\; dA / \int_{A_\infty} \psi\bar{\psi}\; dA \; . \tag{5.3}$$

Equation 5.3 is an exact result, no approximations have been made yet. In the next section we illustrate by example how equation 5.3 is employed to obtain approximate values of $\tilde{\beta}^2$, given that equation 5.1b can be solved exactly. Essentially, the strategy is to approximate ψ in 5.3 and then evaluate the integrals to obtain $\tilde{\beta}^2$.

5.2 Examples of Scalar Perturbation Theory

In this section I use equation 5.3 to obtain some results which are used in Chapter 4.

Example 1: Change in $\tilde{\beta}$ due to a small change in the radius of a circular fiber.

In this problem, using the notation of equations 5.1,

$$k^2 = \begin{cases} k_{co}^2 & r < \rho \\ k_{cl}^2 & r > \rho \end{cases} \tag{5.4a}$$

and

$$\bar{k}^2 = \begin{cases} k_{co}^2 & r < \bar{\rho} \\ k_{cl}^2 & r > \bar{\rho} \end{cases} \tag{5.4b}$$

where $|(\rho-\bar{\rho})/\rho| << 1$. We suppose that $\bar{\tilde{\beta}}$ and $\bar{\psi}$ are known. Because $k^2 \cong \bar{k}^2$, it is plausible that $\psi \cong \bar{\psi}$. In the perturbation region, $\bar{\psi}(r,\phi) \cong \bar{\psi}(\bar{\rho},\phi)$. With these two approximations equation 5.3 becomes

$$\tilde{\beta}^2 = \bar{\tilde{\beta}}^2 + [(k_{co}^2 - k_{cl}^2)\bar{\rho}(\rho-\bar{\rho})\int_o^{2\pi}\bar{\psi}^2(\rho,\phi)d\phi/\int_{A_\infty}\bar{\psi}^2(r,\phi)dA] \qquad (5.5)$$

$$= \bar{\tilde{\beta}}^2 + \{2\tilde{U}^2K_\ell^2(\tilde{W})/\rho^2K_{\ell-1}(\tilde{W})K_{\ell+1}(\tilde{W})\}\cdot\{(\rho-\bar{\rho})/\bar{\rho}\} \qquad (5.6)$$

where equations 3.3, 4.1 and Table 4.1 have been used. The result in equation 5.6 could, of course, also be obtained by differentiating the eigenvalue equation with respect to $\bar{\rho}$. The derivation above is a quicker method of obtaining the same answer.

Example 2: Change in $\tilde{\beta}$ due to a small elliptic deformation of a circular fiber.

This problem is similar to Example 1. Since the deformation is very small we again take $\psi \cong \bar{\psi}$ (in this problem $\bar{\psi}$ is the known solution for a circular fiber). The ellipse departs only slightly from the circular geometry within a crescent shaped region about the x-axis of Figure 3.2, so that $k^2-\bar{k}^2 = \theta_c^2 k_{co}^2$ in this perturbation region and zero elsewhere. The perturbation is close to the circle boundary, so that

$$\bar{\psi}(r,\phi) \cong \psi(r,\phi) \cong \psi(\bar{\rho},\phi) \quad \text{and} \quad dA = 1/2(e\bar{\rho})^2\cos^2\phi$$

in the perturbation region. With these approximations equation 5.3 leads to

$$\text{a) } \ell = 0 : \tilde{\beta}^2 = \bar{\tilde{\beta}}^2 + \{e^2\tilde{U}^2K_o^2(\tilde{W})/\rho^2K_1^2(\tilde{W})\} \qquad (5.7a)$$

$$\text{b) } \ell = 1 \text{ even symmetry} : \tilde{\beta}^2 = \bar{\tilde{\beta}}^2 + \{3e^2\tilde{U}^2K_1^2(\tilde{W})/4\rho^2K_o(\tilde{W})K_2(\tilde{W})\} \qquad (5.7b)$$

$$\ell = 1 \text{ odd symmetry} : \quad \tilde{\beta}^2 = \bar{\tilde{\beta}}^2 + \{e^2\tilde{U}^2K_1^2(\tilde{W})/4\rho^2K_o(\tilde{W})K_2(\tilde{W})\} \tag{5.7c}$$

$$\text{c) } \ell \geq 1 : \quad \tilde{\beta}^2 = \bar{\tilde{\beta}}^2 + o(e^4) \tag{5.7d}$$

In Section 4.3 the difference between the $\tilde{\beta}$'s of the two $\ell = 1$ modes was required. In the notation of that section,

$$\tilde{\beta}_e - \tilde{\beta}_o = (\tilde{\beta}_e^2 - \tilde{\beta}_o^2)/2k_{co} = \theta_c e^2\tilde{U}^2K_1^2(\tilde{W})/4\rho VK_o(\tilde{W})K_2(\tilde{W}) \tag{5.8}$$

which is one of the intermediate steps leading to equation 4.9.

Example 3: Modes of the two parallel nonidentical fibers.

This problem is somewhat different to the preceeding two; a simple approximation such as $\psi = \bar{\psi}$ is no longer possible. In Section 4.4 this problem was discussed for two identical fibers; the familiar symmetric and antisymmetric combinations in equation 4.13 are no longer approximate solutions of

$$\{\nabla^2 + k^2\}\psi = \tilde{\beta}^2\psi \tag{5.9}$$

when the fibers are nonidentical. Instead it is necessary to form a more general linear combination

$$\psi = a_1\bar{\psi}_1 + a_2\bar{\psi}_2 \tag{5.10}$$

where $\bar{\psi}_1$ is a solution of the scalar wave equation of fiber 1 in isolation and $\bar{\psi}_2$ is a solution of the scalar wave

equation of fiber 2 in isolation. Note that

$$\int_{A_\infty} \bar{\psi}_1 \bar{\psi}_2 \, dA \neq 0 \tag{5.11}$$

since $\bar{\psi}_1$ and $\bar{\psi}_2$ are solutions of <u>different</u> scalar wave equations. Now one substitutes equation 5.10 and either $\bar{\psi}_1$ or $\bar{\psi}_2$ into equation 5.3 and obtains a 2 x 2 system of linear equations

$$\{C_{11} + \bar{\tilde{\beta}}_1^2 - \tilde{\beta}^2\}a_1 + \{C_{12} + D_1(\bar{\tilde{\beta}}_1^2 - \tilde{\beta}^2)\}a_2 = 0 \tag{5.12a}$$

$$\{C_{21} + D_2(\bar{\tilde{\beta}}_2^2 - \tilde{\beta}^2)\}a_1 + \{C_{22} + \bar{\tilde{\beta}}_2^2 - \tilde{\beta}^2\}a_2 = 0 \tag{5.12b}$$

where

$$C_{ij} = \int_{A_\infty} (k^2 - \bar{k}_i^2)\bar{\psi}_i \bar{\psi}_j \, dA / \int_{A_\infty} \psi_i^2 \, dA \tag{5.13a}$$

$$D_i = \int_{A_\infty} \psi_1 \psi_2 \, dA / \int_{A_\infty} \psi_i^2 \, dA \; . \tag{5.13b}$$

Equations 5.12 determine $\tilde{\beta}^2$, in addition to a_1/a_2. $\tilde{\beta}^2$ is obtained by equating the determinant of equation 5.12 to zero and solving the resulting quadratic. Once $\tilde{\beta}^2$ is known, a_1/a_2 can be determined from either of equations 5.12. When the term $D_i << 1$, as happens when the fibers are far enough apart or far from cutoff, it can be neglected and the problem discussed in Appendix A is recovered.

We now make several assumptions to simplify the algebra

(a) Assume that $\bar{\tilde{\beta}}_1^2 >> C_{11}$, $\bar{\tilde{\beta}}_2^2 >> C_{22}$ and $|\bar{\tilde{\beta}}_1^2 - \bar{\tilde{\beta}}_2^2| >> |C_{11} - C_{22}|$, so that C_{11} and C_{22} can

be neglected.

(b) Assume that the fibers differ only slightly in radius, so that $C_{12} \cong C_{21} = C$ and $\bar{\tilde{\beta}}_1^2 - \bar{\tilde{\beta}}_2^2$ is given by equation 5.6.

(c) Assume that the fibers are far apart or far from cutoff, so that $D_1, D_2 << 1$ and can be neglected.

As mentioned before, assumption (c) is sufficient to ensure that the results of Appendix A are recovered. Assumptions (a) and (b) are equivalent to the two assumptions leading to equations A.4 and A.5. Hence, from Appendix A,

$$\tilde{\beta}^2 = \{(\bar{\tilde{\beta}}_1^2 + \bar{\tilde{\beta}}_2^2)/2\} \pm C[\Lambda^2 + 1]^{1/2} \tag{5.14}$$

$$a_1/a_2 = \Lambda \pm [\Lambda^2 + 1]^{1/2} \tag{5.15}$$

$$\Lambda = (\bar{\tilde{\beta}}_1^2 - \bar{\tilde{\beta}}_2^2)/2C \ . \tag{5.16}$$

The quantity C is given in reference 1, one has

$$C = \tilde{U}^2\{K_{2\ell}(\tilde{W}d/\rho) + K_o(\tilde{W}d/\rho)\}/\rho^2V^2K_{\ell-1}(\tilde{W})K_{\ell+1}(\tilde{W}) \tag{5.17a}$$

if $\bar{\psi}_1 = f_\ell(r_1)\cos\ell\phi_1$, $\bar{\psi}_2 = f_\ell(r_2)\cos\ell\phi_2$ and

$$C = \tilde{U}^2\{(-)^\ell K_{2\ell}(\tilde{W}d/\rho) + K_o(\tilde{W}d/\rho)\}/\rho^2V^2K_{\ell-1}(\tilde{W})K_{\ell+1}(\tilde{W}) \tag{5.17b}$$

if $\bar{\psi}_1 = f_\ell(r_1)\sin\ell\phi_1$, $\bar{\psi}_2 = f_\ell(r_2)\sin\ell\phi_2$. Since the radii of the two fibers are nearly equal, $\bar{\tilde{\beta}}_1^2 - \bar{\tilde{\beta}}_2^2$ is given by equation 5.6,

$$\bar{\tilde{\beta}}_1^2 - \bar{\tilde{\beta}}_2^2 = \{2\tilde{U}^2K^2(\tilde{W})/\rho^2(K_{\ell-1}(\tilde{W})K_{\ell+1}(\tilde{W})\}\{\delta\rho/\rho\} \ . \qquad (5.18)$$

Equation 5.17 and 5.18 are used to calculate Λ (equation 5.16). For example, when $\ell = 0$,

$$\Lambda = \{V^2K_o^2(\tilde{W})/2K_o(\tilde{W}d/\rho)\}\{\delta\rho/\rho\} \ . \qquad (5.19)$$

Note how the answer reduces to the symmetric and anti-symmetric combinations in equation 4.13 when $\delta\rho = 0$. Equations 4.15 follow from equations 5.14 and 5.17a.

5.3 Vector Perturbation Theory

Sections 5.3 and 5.4 are a digression from the mainstream of this thesis. In these two sections a method for perturbing about a known solution of Maxwell's equations is presented This method is similar to those in references 2 and 5, though more general.

Consider two different modal solutions of Maxwell's equations

(a) $\underline{E}(x,y,z) = \underline{e}(x,y)e^{i\beta z}$, $\underline{H}(x,y,z) = \underline{h}(x,y)e^{i\beta z}$ corresponding to an electric permittivity $\varepsilon(x,y)$.

(b) $\underline{\bar{E}}(x,y,z) = \underline{\bar{e}}(x,y)e^{i\bar{\beta} z}$, $\underline{\bar{H}}(x,y,z) = \underline{\bar{h}}(x,y)e^{i\bar{\beta} z}$ corresponding to an electric permittivity $\bar{\varepsilon}(x,y)$.

Using the curl equations and well known vector identities it is easily shown that if

$$\underline{F} = \underline{E} \times \bar{\underline{H}}^* + \bar{\underline{E}}^* \times \underline{H} \tag{5.20}$$

then

$$\nabla \cdot \underline{F} = -i\omega\{\bar{\varepsilon} - \varepsilon\}\, \underline{E} \cdot \bar{\underline{E}}^* \ . \tag{5.21}$$

Integrating equation 5.21 over the whole plane and using the two dimensional Gauss theorem

$$\partial/\partial z \int_{A_\infty} \hat{z} \cdot \underline{F}\, dA = \int_{A_\infty} \nabla \cdot \underline{F}\, dA \tag{5.22}$$

one has

$$\beta - \bar{\beta} = \omega \int_{A_\infty} (\varepsilon - \bar{\varepsilon})\, \underline{e} \cdot \bar{\underline{e}}\, dA \Big/ \int_{A_\infty} (\underline{e} \times \bar{\underline{h}}^* + \bar{\underline{e}}^* \times \underline{h}) \cdot \hat{z}\, dA \ . \tag{5.23}$$

Equation 5.23 is an exact result, no approximations have been made yet. In the next section we illustrate by example how equation 5.23 is employed to obtain approximate values of β, given that $\bar{\underline{E}}$, $\bar{\underline{H}}$ and $\bar{\beta}$ are known.

5.4 Examples of Vector Perturbation Theory

1. Elliptic Deformation of the Core of a Step Index Fiber

The consequences of an elliptic deformation of a step-index waveguide have already been discussed in Section 4.3. Recall that in order to apply the $n_{co} \cong n_{cl}$ method one must first solve the scalar wave equation for an elliptic fiber. The $n_{co} \cong n_{cl}$ method is not restricted to slightly deformed

circles, ellipses with arbitrary eccentricity can be treated provided one is willing to manipulate the Mathieu functions which arise from the scalar equation. In this subsection we avoid doing this by using the results of Section 5.3 to perturb around the exact modes of a circular step index waveguide. This second method requires that the eccentricity of the ellipse is small, however it does not require that $n_{co} \cong n_{cl}$.

The fundamental modes are discussed first (see Section 3.2(1) and 4.3(2)). I shall calculate the difference in the modal propagation constants, $\beta_x - \beta_y$, using equation 5.23. The quantities $\bar{E}$, $\bar{H}$ and $\bar{\beta}$ are the modal quantities associated with the circular fiber. Since the deformation is small we let $\underline{e} = \underline{\bar{e}}$ and $\underline{h} = \underline{\bar{h}}$ in equation 5.23 and then calculate β. The integrals over the crescent shaped perturbation region is evaluated as in Section 5.2(2).

For example, consider the predominantly x-polarised fundamental mode. For the present I shall write the electric field of this mode as

$$\underline{\bar{e}} = g_r(r)\cos\phi\ \hat{\underline{r}} - g_\phi(r)\sin\phi\ \hat{\underline{\phi}} - i\theta_c g_z(r)\cos\phi\ \hat{\underline{z}} \qquad (5.24a)$$

$$= \{f_o(r)\hat{\underline{x}} + O(\theta_c^2)\} - i\theta_c g_z(r)\cos\phi\ \hat{\underline{z}}\ . \qquad (5.24b)$$

Expressions for g_r, g_ϕ and g_z are given in references 4 and 6. Unfortunately equation 5.24b is not sufficiently accurate for our purposes, the order θ_c^2 corrections to the transverse field give rise to an important contribution to $\beta_x - \beta_y$. Substituting $\underline{e}(r,\phi) = \underline{\bar{e}}(r,\phi) = \underline{\bar{e}}(\rho,\phi)$ and $dA = 1/2(e\bar{\rho})\cos^2\phi$

into 5.23 gives

$$\beta_x = \bar{\beta} + \omega\varepsilon_{co}(e\bar{\rho}\theta_c)^2\{g_r^2(\bar{\rho}) + 3g_\phi^2(\bar{\rho}) + \theta_c^2 g_z^2(\bar{\rho})\}/16\int_{A_\infty} \underline{\bar{e}} \times \underline{\bar{h}}^* \cdot \hat{z}\, dA \tag{5.25}$$

Similarly for the predominantly y-polarised fundamental mode

$$\beta_y = \bar{\beta} + \omega\varepsilon_{co}(e\bar{\rho}\theta_c)^2\{3g_r^2(\bar{\rho}) + g_\phi^2(\bar{\rho}) + 3\theta_c^2 g_z^2(\bar{\rho})\}/16\int_{A_\infty} \underline{\bar{e}} \times \underline{\bar{h}}^* \cdot \hat{z}\, dA \tag{5.26}$$

From equations 5.25 and 5.26

$$\beta_x - \beta_y = \omega\varepsilon_{co}(e\bar{\rho}\theta_c)^2\{g_\phi^2(\bar{\rho}) - g_r^2(\bar{\rho}) - \theta_c^2 g_z^2(\bar{\rho})\}/8\int_{A_\infty} \underline{\bar{e}} \times \underline{\bar{h}}^* \cdot \hat{z}\, dA \tag{5.27a}$$

$$= \{\omega\varepsilon_{co}(e\bar{\rho}\theta_c)^2\{g_\phi^2(\bar{\rho}) - g_r^2(\bar{\rho}) - \theta_c^2 g_z^2(\bar{\rho})\}/16\int_o^\infty dr\ r f_o^2(r) + O(\theta_c^4) \tag{5.27b}$$

where $g_r(r) + O(\theta_c^2) = g_\phi(r) + O(\theta_c^2) = f_o(r)$ has been used in the transition from equation 5.27a to 5.27b. The integral in equation 5.27b is listed in Table 4.1, $g_\phi^2(\bar{\rho}) - g_r^2(\bar{\rho})$ can be calculated from the material in reference 4. The final result, which was quoted previously in equation 4.10, is

$$\beta_x - \beta_y = e^2\theta_c^3\tilde{U}^2\tilde{W}^2\{1 + (\tilde{U}K_o^2(\tilde{W})J_2(\tilde{U})/K_1^2(\tilde{W})J_1(\tilde{U}))\}/8\rho V^3 \ . \tag{5.28}$$

This result does not agree with an earlier calculation by Marcuse,[5] to obtain Marcuse's result replace the curly-

bracketed term in equation 5.28 by unity. This significant difference is due to Marcuse's neglect of $g_r^2(\bar{\rho}) - g_\phi^2(\bar{\rho})$ in equation 5.27b. Clearly this term is of the same order as the term he retained viz $\theta_c^2 g_z^2(\bar{\rho})$.

Equation 5.23 can also be used to investigate the higher order modes of a slightly elliptic fiber, the results of Section 4.3 are easily recovered. For the higher order modes (in this case the $\ell = 1$ modes) one is primarily interested in determining the composition of the modes as the parameters defining the waveguide, e and V, are altered. (This has been done previously using the $n_{co} \cong n_{cl}$ method and the answer is contained in equations 3.7, 3.9 and 4.9.) We know from the discussion in Section 3.2 that an elliptic perturbation hybridises or mixes the HE_{even} mode with the TM mode and the HE_{odd} mode with the TE mode. Thus a plausible candidate for the electric field of an ellipse mode is

$$\underline{e}_i = a_{i1}^{i}\bar{\underline{e}}_1 + a_{2}^{i}\bar{\underline{e}}_2 \quad (i = 1,2) \tag{5.29}$$

where $\bar{\underline{e}}_1$ and $\bar{\underline{e}}_2$ are the TM and HE_{even} electric fields respectively (the superscript $^-$ has been used for consistency with equation 5.23). The analogy between equations 3.7 and 5.29 is clear; in both equations an ellipse mode is represented as a linear combination of unperturbed modes.[6] The ratio a_1^i/a_2^i in equation 5.29 (which clearly equals $\{(a_{ex}^i/a_{oy}^i) + 1\}/\{(a_{ex}^i/a_{oy}^i) - 1\}$, from equation 3.5 and 3.7) is obtained by substituting equation 5.29 and either $\bar{\underline{e}}_1$ or $\bar{\underline{e}}_2$ into equation 5.23 and then solving the resulting 2 x 2 eigenvalue problem using the results of Appendix A. The

result is

$$a_1^i/a_2^i = \Lambda' \pm (\Lambda'^2 + 1)^{1/2} \tag{5.30}$$

$$\Lambda' = 1/\Lambda \tag{5.31}$$

$$= (\beta_1-\beta_2)/(\tilde{\beta}_e-\tilde{\beta}_o) \tag{5.31b}$$

where Λ is given by equations 3.13, 4.9. It is easily shown from 5.30 and $a_1^i/a_2^i = \{(a_{ex}^i/a_{oy}^i) + 1\}/\{(a_{ex}^i/a_{oy}^i) - 1\}$ that

$$a_{ex}^i/a_{oy}^i = \Lambda \pm (\Lambda^2 + 1)^{1/2} \tag{5.32}$$

in agreement with equation 3.9. Thus the two theories agree when $\theta_c << 1$ and $e << 1$, as expected.

2. Two Parallel Step Index Fibers

This problem is discussed in reference 2 using equation 5.23 and from the previous example it is clear that results consistent with those of Section 4.4(2) will be obtained.

Bibliography and Footnotes for Chapter 5

1. P.D. McIntyre and A.W. Snyder, "Power transfer between optical fibers," J. Opt. Soc. Am. 63(12), 1518-1527 (1973).

2. A.W. Snyder, "Coupled mode theory for optical fibers," J. Opt. Soc. Am. 62, 1268-1277 (1972).

3. A.W. Snyder, "Mode propagation in optical waveguides," Elect. Lett. 6(18), (1970).

4. A.W. Snyder, "Asymptotic expressions for eigenfunctions and eigenvalues of dielectric or optical waveguides," IEEE trans. MTT 17, 1130-1138 (1969).

5. D. Marcuse, Theory of Dielectric Optical Waveguides, Academic Press, New York (1974).

6. In equation 3.7 the unperturbed modes are $n_{co} = n_{cl}$ fields (with arbitrary eccentricity), the perturbation is nonzero θ_c (i.e., polarisation dependent effects). In equation 5.29 the unperturbed modes are circle fields (with arbitrary n_{co} and n_{cl}), the perturbation is nonzero eccentricity. When both e and $\theta_c << 1$, both theories give equivalent results.

APPENDIX A

SOLVING THE 2 x 2 EIGENVALUE PROBLEM

An essential step in the application of the perturbation theories in this thesis is the solution of the 2 x 2 eigenvalue problem. For convenience, the details of the algebra as well as some remarks about the properties of the solution have been collected in this appendix.

Recall that the basic strategy of the Rayleigh-Schrödinger perturbation theory[1] is to approximate a mode of the perturbed system by a linear combination of modes of the unperturbed system. The unknown coefficients in the linear combination, a_1 and a_2, and the propagation constant of the perturbed mode, β, are obtained from the 2 x 2 eigenvalue problem

$$\begin{bmatrix} C_{11} + \beta_1^2 - \beta^2 & C_{12} \\ C_{21} & C_{22} + \beta_2^2 - \beta^2 \end{bmatrix} \begin{bmatrix} a_1 \\ a_2 \end{bmatrix} = 0 \qquad \text{(A.1)}$$

The definitions of C_{ij} and β_i depend on which theory is being applied. Equation A.1 is a system of linear homogeneous equations. For a nontrivial solution to exist the determinant of the system must be zero.[1] Equating the determinant to zero and rearranging one obtains a quadratic equation for the eigenvalue β^2

$$\beta^2 - \{C_{11} + \beta_1^2 + C_{22} + \beta_2^2\}\beta + \{(C_{11} + \beta_1^2)(C_{22} + \beta_2^2) - C_{12}C_{21}\} = 0 \; . \qquad \text{(A.2)}$$

The solutions of this quadratic are

$$\beta_{\pm}^2 = [\{C_{11} + \beta_1^2 + C_{22} + \beta_2^2\}/2] \pm [\{C_{11} + \beta_1^2 - C_{22} - \beta_2^2\}^2 + C_{12}C_{21}]^{1/2} . \quad (A.3)$$

Once β^2 has been obtained, equation A.1 is used to calculate a_2/a_1. This completes the discussion of the general solution of equation A.1.

In many problems the results above can be further simplified because

a) $\beta_1^2 >> C_{11}$, $\beta_2^2 >> C_{22}$ and $|\beta_1^2 - \beta_2^2| >> |C_{11} - C_{22}|$, hence C_{11} and C_{22} are neglected throughout.

b) $C_{12} \cong C_{21}$, hence C_{12} and C_{21} are both replaced by C throughout.

Note that because of (b) the perturbation matrix is symmetric and consequently the eigenvectors are perpendicular. With approximations (a) and (b) the solutions of equation A.1 can be written as

$$\beta_+^2 = [\{\beta_1^2 + \beta_2^2\}/2] + C[1 + \Lambda^2]^{1/2} \quad (A.4a)$$

$$a_1^+/a_2^+ = \Lambda + [1 + \Lambda^2]^{1/2} \quad (A.4b)$$

and

$$\beta_-^2 = [\{\beta_1^2 + \beta_2^2\}/2] - C[1 + \Lambda^2]^{1/2} \quad (A.4c)$$

$$a_1^-/a_2^- = \Lambda - [1 + \Lambda^2]^{1/2} \quad (A.4d)$$

where

$$\Lambda = (\beta_1^2 - \beta_2^2)/2C \quad . \tag{A.5}$$

When the approximations (a) and (b) are made the composition of the perturbed modes (i.e., the ratio a_1/a_2) depends only on the important parameter Λ.

The physical significance of the above solution is best appreciated if we consider a particular problem. Suppose, for example, that an unperturbed mode is excited at z = 0 on the perturbed structure. The subsequent development of the field is analyzed using the modal expansion method described in Chapter 1; the unperturbed mode is expanded in terms of the true modes of the structure using equations A.4b and A.4d.

In the scalar perturbation theory of Chapter 5, for example, let ψ_+ and ψ_- be the modes of the perturbed system and ψ_1 and ψ_2 be the modes of the unperturbed system. Apparently

$$\psi_+ = a_1^+\psi_1 + a_2^+\psi_2 \tag{A.6a}$$

and

$$\psi_- = a_1^-\psi_1 + a_2^-\psi_2 \quad . \tag{A.6b}$$

If ψ_1 is excited at z = 0, the field at $z \neq 0$ is given by:

$$\{a_2^-\psi_+ e^{i\beta_+ z} - a_2^+\psi_- e^{i\beta_- z}\}/\{a_1^+a_2^- - a_2^+a_1^-\} \tag{A.7}$$

$$= \{(a_1^+a_2^- e^{i\beta_+ z} - a_2^+a_1^- e^{i\beta_- z})/(a_1^+a_2^- - a_2^+a_1^-)\}\psi_1$$

$$+ \{a_2^-a_2^+/(a_1^+a_2^- - a_2^+a_1^-)\}\{e^{i\beta_+ z} - e^{i\beta_- z}\}\psi_2 \tag{A.8}$$

$$= A_1(z)\psi_1 + A_2(z)\psi_2 \ . \qquad \text{(A.9)}$$

Note that since $A_1(0) = 1$ and $A_2(0) = 0$ the initial conditions are satisfied. In equation A.9, the field at $z \neq 0$ has been cast into the form favoured by coupled mode theory.[2] The power in modes 1 and 2 is proportional to the quantities

$$|A_1(z)|^2 = 1 - F \sin^2[(\beta_+ - \beta_-/2)z] \qquad \text{(A.10a)}$$

$$|A_2(z)|^2 = F \sin^2[(\beta_+ - \beta_-/2)z] \qquad \text{(A.10b)}$$

where

$$F = [1 + \Lambda^2]^{-1} \ . \qquad \text{(A.11)}$$

All the power starts in mode 1 and a fraction F is then exchanged periodically between the two unperturbed modes ψ_1 and ψ_2. The beatlength

$$L = 2\pi/|\beta_+ - \beta_-| \qquad \text{(A.12)}$$

is the length over which the fraction F is transferred from mode 1 to mode 2 and back again. The fraction F depends on the important parameter Λ; when $\Lambda >> 1$ essentially all the energy stays in the unperturbed mode 1, when $\Lambda = 0$ all the energy is periodically exchanged between the two unperturbed modes.

In conclusion, the parameter Λ defined in equation A.5 determines two important physical quantities

a) the composition of the perturbed modes in terms of the unperturbed modes through equations A.4b and A.4d;

b) the fraction of power periodically exchanged between two unperturbed modes through equations A.10 and A.11.

Bibliography for Appendix A

1. C.A. Croxton, Introductory Eigenphysics: An Approach to the Study of Fields, London, New York, Wiley (1974).

2. W.H. Louisell, Coupled Mode and Parametric Electronics, Wiley, New York (1960).

APPENDIX B

CORRECTION OF $\tilde{\beta}$ FROM THE EXACT EIGENVALUE EQUATION

In Section 4.1 the $\tilde{\beta}$ of the circular step-index waveguide was corrected using equation 2.12. In this appendix I prove, using the exact eigenvalue equation,[1,2] that the corrected β's are exact to order θ_c^3 (i.e., terms of order θ_c^5 have been neglected).

First I prove an important general result. Suppose that the solution of the transcendental equation

$$f(x) = g(x) \tag{B.1}$$

is known (f and g are initially well behaved functions). How can the knowledge be used to obtain an approximate solution of

$$(1 + \varepsilon)f(x) = g(x) \tag{B.2}$$

when $\varepsilon << 1$? Equation B.2 defines x as a function of ε implicitly. Differentiating equation B.2 with respect to ε, setting $\varepsilon = 0$ and solving for $dx(0)/d\varepsilon$ leads to

$$dx(0)/d\varepsilon = f(x(0))/\{g'(x(0)) - f'(x(0))\} \tag{B.3}$$

where ' indicates differentiation with respect to argument. The number x(0) in equation B.3 is known, since by assumption equation B.1 can be solved exactly. Hence, since $\varepsilon << 1$,

$$x(\varepsilon) = x(0) + \varepsilon dx(0)/d\varepsilon + 0(\varepsilon^2) \tag{B.4}$$

where x(0) is known from equation B.1 and dx(0)/dε is known from equation B.3.

Now $\tilde{\beta}$, which is considered known, is defined implicitly by the equations

$$J_{\ell-1}(\tilde{U})/\tilde{U}J_{\ell}(\tilde{U}) = K_{\ell-1}(\tilde{W})/\tilde{W}K_{\ell}(\tilde{W})$$

or equivalently

$$J_{\ell+1}(\tilde{U})/\tilde{U}J_{\ell}(\tilde{U}) = -K_{\ell+1}(\tilde{W})/\tilde{W}K_{\ell}(\tilde{W}) \qquad \text{(B.5)}$$

$$(\rho\tilde{\beta})^2 = (\rho k_{co})^2 - \tilde{U}^2 = (\rho k_{c1})^2 + \tilde{W}^2 \ . \qquad \text{(B.6)}$$

$\tilde{\beta}$ is an approximation of β which ignores terms of order θ_c^3. Gloge has shown[3] that to obtain a more accurate approximation of β, which ignores terms of order θ_c^5, equation B.5 must be replaced by

a) For the TM mode: $J_1(U)/UJ_o(U) = -(1+\theta_c^2)K_1(W)/WK_o(W)$ (B.7a)

b) For the $EH_{\ell-1}$ modes:

$$J_{\ell}(U)/UJ_{\ell-1}(U) = -(1+(1/2)\theta_c^2)K_{\ell}(W)/WK_{\ell-1}(W) \quad (\ell \neq 1) \qquad \text{(B.7b)}$$

c) For the $HE_{\ell+1}$ modes:

$$J_{\ell}(U)/UJ_{\ell+1}(U) = (1+(1/2)\theta_c^2)K_{\ell}(W)/WK_{\ell+1}(W) \qquad \text{(B.7c)}$$

d) For the TE modes: $J_1(U)/UJ_o(U) = -K_1(W)/WK_o(W)$. (B.7d)

Note how if one ignores terms of order θ_c^2 compared to 1 in equation B.7, equation B.5 is recovered. Also, the degeneracies between EH and HE modes in equation B.5 have been removed in equation B.7.

The analogy between equations B.5, B.7 and equations B.1, B.2 is clear. For example, consider the TM mode, then

$$g = J_1/UJ_o \tag{B.8a}$$

$$f = -K_1/WK_o \tag{B.8b}$$

$$\varepsilon = \theta_c^2 \tag{B.8c}$$

$$x = \beta^2 \tag{B.8d}$$

$$x(0) = \tilde{\beta}^2 \tag{B.8e}$$

$$dx(0)/d\varepsilon = d(\beta^2(0)/d(\theta_c^2). \tag{B.8f}$$

The quantity $d\beta^2(0)/d(\theta_c^2)$ is obtained mutatis mutandis from equation B.3,

$$d\beta^2(0)/d\theta_c^2 = -K_1(\tilde{W})/2\rho^2\tilde{W}K_o(\tilde{W})\{1/\tilde{W}\ d/d\tilde{W}(K_1(\tilde{W})/\tilde{W}K_o(\tilde{W}))$$

$$- 1/\tilde{U}\ d/d\tilde{U}(J_1(\tilde{U})/\tilde{U}J_o(\tilde{U}))\} \tag{B.10}$$

$$= -2\tilde{U}^2\tilde{W}K_1(\tilde{W})/\rho^2V^2K_2(\tilde{W}) \tag{B.11}$$

where the eigenvalue equation and standard Bessel function

identities have been used. From equation B.11,

$$\beta^2 = \tilde{\beta}^2 - \{2\theta_c^2\tilde{U}^2\tilde{W}K_1(\tilde{W})/\rho^2V^2K_2(\tilde{W})\} + O(\theta_c^4) \qquad \text{(B.12)}$$

which agrees with the correction obtained from equation 2.12. The other corrections obtained from equation 2.12 can be verified similarly.

Bibliography for Appendix B

1. A.W. Snyder, "Asymptotic expressions for eigenfunctions and eigenvalues of dielectric or optical waveguides," IEEE trans. MTT 17, 1130-1138 (1969).

2. D. Marcuse, Light Transmission Optics, Van Nostrand Reinhold, Princeton, New Jersey (1972).

3. D. Gloge, "Weakly guiding fibers," Appl. Opt. 10, 2252-2258 (1971).

APPENDIX C

THE PROPAGATION CONSTANTS OF THE FUNDAMENTAL MODES OF THE TWO FIBER SYSTEM - DETAILS OF THE ALGEBRA

The four fundamental modes of the two fiber system are given in equation 4.16. $\tilde{\beta}_+$ and $\tilde{\beta}_-$ are corrected using equation 2.12 with $\underline{\tilde{e}}_t = \underline{e}_t = \underline{e}_{x+}$ and so on for the remaining three modes. Taking $\underline{e}_{x+}$, for example, and using equation 2.14 one has

$$\beta_{x+}^2 = \tilde{\beta}_+^2 + \theta_c^2\{\oint_{\text{Boundary}}\psi_+(\nabla\psi_+ \cdot \hat{x})(\hat{n} \cdot \hat{x})\,d\ell / \int_{A_\infty}\psi_+^2\,dA\} \quad (C.1)$$

where the line integral is over both circles in Figure 3.2. Clearly the contribution of each circle is equal and so

$$\oint_{\text{Boundary}}\psi_+(\nabla\psi_+ \cdot \underline{\hat{x}})(\hat{n} \cdot \underline{\hat{x}})\,d\ell = 2[\oint_{\text{Circle 1}}(\hat{n} \cdot \underline{\hat{x}})\{\psi_1(\nabla\psi_1 \cdot \underline{\hat{x}}) + \psi_2(\nabla\psi_1 \cdot \hat{x}) + \psi_1(\nabla\psi_2 \cdot \underline{\hat{x}})\}d\ell] \quad (C.2)$$

where the term containing two evanescent functions has been neglected. The first term on the right hand side of equation C.2 has been evaluated previously; it is the polarisation correction to $\tilde{\beta}$ of an isolated fiber (see Section 4.1 and Table 4.1). The remaining two integrals are evaluated using

$$K_o(\tilde{W}r_1/\rho) = \sum_{\ell=-\infty}^{\infty}(-)^\ell \cos\ell\phi_2 I_\ell(\tilde{W}r_2/\rho)K_\ell(\tilde{W}d/\rho) \quad (C.3)$$

where r_1, r_2 and ϕ_2 are defined in Figure 3.2. Only the $\ell = 0$ and $\ell = 2$ terms survive the integration. The integral

in the denominator of equation C.1 is evaluated elsewhere[1]; it is assumed that $\int_{A_\infty} \psi_1 \psi_2 \, dA$ is negligible.

Bibliography for Appendix C

1. A.W. Snyder, "Asymptotic expressions for eigenfunctions and eigenvalues of a dielectric or optical waveguide," IEEE MTT-17(12), 1130-1138 (1969).

BIBLIOGRAPHY

Adler, R.B., "Waves on inhomogeneous cylindrical structures," Proc. IRE 40, 339-348 (1952).

Adler, R.B., "Properties of guided waves on inhomogeneous cylindeical structures," M.I.T. Research Lab. of Electronics, Tech. Report 102 (1949).

Born, M. and Wolf, E., Principles of Optics, 3rd Edition, Pergamon Press, New York (1964).

Carson, J., Mead, S., Schelkunoff, S., "Hyper frequency wave guides - mathematical theory," BSTJ 15 (1936).

Chandler, C.H., "An investigation of dielectric rods as waveguides," J. Appl. Phys. 20 (1949).

Clarricoats, P.J.B., "Theory of optical fiber waveguides: a review" in Progress in Optics, Vol. 14, E. Wolf (ed.) (North Holland, Amsterdam, 1976).

Croxton, C.A., Introductory Eigenphysics: An Approach to the Theory of Fields, London, New York, Wiley (1974).

Enoch, J.M., "Optical properties of the retinal receptors," J. Opt. Soc. Am. 53, 71-85 (1963).

Enoch, J.M., "Nature of the transmission of energy in the retinal receptors," J. Opt. Soc. Am. 51, 1122-1126 (1961).

French, W.G. and Tasker, G.W., "Fabrication of graded index and single mode fibers with silica cores," Paper TuA2, OSA/IEEE Meeting on Optical Fiber Transmission, Williamsburg (1975).

Gloge, D., "Weakly guiding fibers," Appl. Opt. 10(10), 2252-2258 (1971).

Kao, K.C. and Hockham, G.A., "Dielectric-fiber surface waveguides for waveguides," Proc. IRE 113(7), 1151 (1966).

Kapany, N.S. and Burke, J., "Fiber optics in waveguide effects," J. Opt. Soc. Am. 51, 491-498 (1961).

Kapany, N.S. and Burke, J.J., Optical Waveguides, Academic Press, New York (1972).

Kapron, F.P., Keck, D.B. and Maurer, R.D., "Radiation losses in glass optical waveguides," Appl. Phys. Lett. 10, 423-425 (1970).

Koshi, J.O. and Okamoto, K., "Analysis of wave propagation in inhomogeneous optical fibers using a variational method," IEEE trans MTT 22, 938-945 (1974).

Kurtz, C.N., "Scalar and vector mode relations in gradient-index light guides," J. Opt. Soc. Am. 65, 1235-1240 (1975).

Landau, L.D. and Lifshitz, E.M., Electrodynamics of Continuous Media, Pergamon Press (1963).

Louisell, W.H., Coupled Mode and Parametric Electronics, Wiley, New York, 1960.

Marcuse, D., Light Transmission Optics, Van Nostrand Reinhold, Princeton, New Jersey (1972).

Marcuse, D., Theory of Dielectric Optical Waveguides, Academic Press, New York (1974).

McIntyre, P.D. and Snyder, A.W., "Power transfer between optical fibers," J. Opt. Soc. Am. 63(12), 1518-1527 (1973).

Merzbacher, E., Quantum Mechanics, 2nd ed., Wiley, 1970.

Morse, P.M. and Feshbach, H., Methods of Theoretical Physics, McGraw Hill, New York (1953).

Newton, I., Opticks, 4th edition (1730), [Reprinted by Dover, New York (1952).]

Payne, D.N. and Gambling, W.A., "New silica-based low-loss optical fibre," Electron. Lett. 10, 289-290 (1974).

Rayleigh, J.W.S., "Vibrations in dielectric cylinders," Phil. Mag. 43(125), (1897).

Rayleigh, J.W.S., The Theory of Sound, 2 Vols., 2nd ed., Macmillan and Co., London (1894, 1896).

Schawlow, A.L. and Townes, C.H., "Infrared and optical masers," Phys. Rev. 112 (1958).

Snitzer, E. and Osterberg, H., "Observed dielectric waveguide modes of the visible spectrum," J. Opt. Soc. Am. 51, 499-505 (1961).

Snitzer, E., "Cylindrical dielectric waveguide modes," J. Opt. Soc. Am. 51, 499-505 (1961).

Snyder, A.W. and Menzel (eds.), Photoreceptor Optics (Springer-Verlag, Berlin, 1975).

Snyder, A.W., "Asymptotic expressions for eigenfunctions and eigenvalues of a dielectric or optical waveguide," IEEE MTT-17(12), 1130-1138 (1969).

Snyder, A.W. and Pask, C., "Light absorption in the bee photoreceptor," J. Opt. Soc. Am., 62, 998-1008 (1972).

Snyder, A.W., "Mode propagation in optical waveguides," Elect. Lett. 6(18), (1970).

Snyder, A.W., "Coupled mode theory for optical fibers," J. Opt. Soc. Am. 62, 1268-1277 (1972).

Toraldo di Francia, "Per una teoria dell'effecto Stiles-Crawford," Il Nuovo Cimento (9) 5, 589-590 (1948).

Yamada, R. and Inabe, Y., "Guided waves in an optical square-law medium," J. Opt. Soc. Am. 64, 964-969 (1974).